Wind Effects on the Lateral Motion of Wake Vortices

David C. Burnham
James N. Hallock

Research and
Special Programs
Administration
John A. Volpe National
Transportation Systems Center
Cambridge, MA 02142-1093

Final Report
November 1999

This document is available to the public
through the National Technical Information
Service, Springfield, VA 22161

U.S. Department of Transportation
Federal Aviation Administration

19991129 021

DTIC QUALITY INSPECTED 4

REPORT DOCUMENTATION PAGE

Form Approved
OMB No. 0704-0188

1. AGENCY USE ONLY (Leave blank)	2. REPORT DATE November 1999	3. REPORT TYPE AND DATES COVERED Final Report January 1975-December 1984

4. TITLE AND SUBTITLE
Wind Effects on the Lateral Motion of Wake Vortices

6. AUTHOR(S)
David C. Burnham* and James N. Hallock

5. FUNDING NUMBERS
FA927/A9433

7. PERFORMING ORGANIZATION NAME(S) AND ADDRESS(ES)
U.S. Department of Transportation
Research and Special Programs Administration
John A. Volpe National Transportation Systems Center
Cambridge, MA 02142-1093

8. PERFORMING ORGANIZATION REPORT NUMBER
DOT-VNTSC-FAA-99-14

9. SPONSORING/MONITORING AGENCY NAME(S) AND ADDRESS(ES)
U.S. Department of Transportation
Office of Aviation Research
800 Independence Avenue, SW
Washington, DC 20591

10. SPONSORING/MONITORING AGENCY REPORT NUMBER
DOT/FAA/AAR-99/88

11. SUPPLEMENTARY NOTES
*Scientific & Engineering, Inc.
Orleans, MA

12a. DISTRIBUTION/AVAILABILITY STATEMENT
This document is available to the public through the National Technical Information Service, Springfield, VA 22161

12b. DISTRIBUTION CODE

13. ABSTRACT (Maximum 200 words)

This report examines the influence of crosswind and other factors on the behavior of wake vortices. Data from acoustic remote sensors and in situ sensors were used to track the possible transport of wake vortices between parallel runways. The measurements used in the analysis came from landing (1976-7) and takeoff (1980) operations at O'Hare International Airport. As expected, wake vortices are observed to transport with the ambient wind; therefore, dangerous wake vortex encounters can be avoided on parallel runways with suitable assignment of aircraft to the two runways. The analyses of the report were carried out in the mid 1980s and serve to document the O'Hare landing and takeoff databases and how they can be used. The status of the acoustic and in situ wake vortex sensors is updated to the late 1990s.

14. SUBJECT TERMS
wake vortices, parallel runways, crosswind

15. NUMBER OF PAGES
70

16. PRICE CODE

17. SECURITY CLASSIFICATION OF REPORT	18. SECURITY CLASSIFICATION OF THIS PAGE	19. SECURITY CLASSIFICATION OF ABSTRACT	20. LIMITATION OF ABSTRACT
Unclassified	Unclassified	Unclassified	

PREFACE

The present method of preventing strong wake vortex encounters is to increase aircraft separations on arrival and departure behind Heavy aircraft. These increased separations result in a loss in airport capacity. Previous studies of the duration of the wake vortex hazard have shown that the present separation standards are overly conservative most of the time. The possibility of regaining lost airport capacity has thus been one driving force behind the extensive efforts of the U. S. Department of Transportation to understand the behavior of wake vortices. Data on the decay of wake vortices have also been used to increase separation standards to meet required safety levels and to examine possible reclassification of aircraft according to their measured wake vortex properties. Data on wake vortices from landing aircraft have been collected at Kennedy, Denver, Heathrow, and O'Hare airports. Data from aircraft taking off were collected at the Toronto and O'Hare airports.

Two wake-vortex sensors, the Ground-Wind Vortex Sensing System (GWVSS) and the Monostatic Acoustic Vortex Sensing System (MAVSS) were used to collect most of the available wake-vortex data, including the O'Hare airport data used in this report (landing in 1976-7 and takeoff in 1980). The GWVSS was used more extensively, but the MAVSS had the advantage of measuring vortex strength. In 1984 the John A. Volpe National Transportation Systems Center (Volpe Center) completed two draft studies of vortex lateral transport, the first using GWVSS data alone and the second analyzing the MAVSS data collected concurrently; only the second study has been published (1994). The present study extends the analysis of the prior studies to examine how the crosswind affects lateral transport. Such information may lead to improved independent parallel runway separation standards and an algorithm for a parallel-runway dynamic spacing system, such has been under development in Germany since the mid 1980s.

The original database generation and data analysis were carried out by Tom Talbot and Alan Wright of the System Development Corporation and Joe Yarmus, a Volpe Center employee. The current report is based on an April 1986 draft. Since the 1986 figures were not suitable for current publication, the analysis has been repeated in simplified form using the current format of the databases, which was generated by George Ackerman in 1993. This report provides the first published description of the O'Hare databases.

English units are used to describe the test layout in this report. Calculated quantities such as vortex strength are presented in metric units.
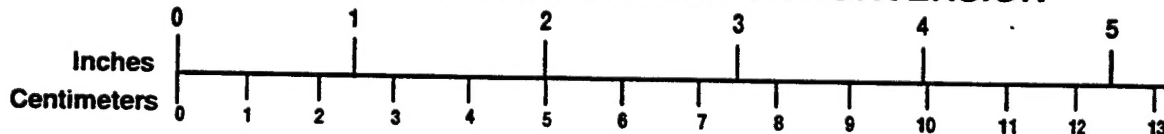
iii

METRIC/ENGLISH CONVERSION FACTORS

ENGLISH TO METRIC
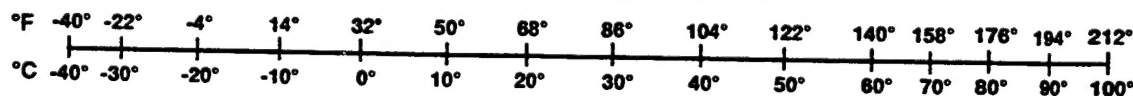
LENGTH (APPROXIMATE)

1 inch (in) = 2.5 centimeters (cm)

1 foot (ft) = 30 centimeters (cm)

1 yard (yd) = 0.9 meter (m)

1 mile (mi) = 1.6 kilometers (km)

AREA (APPROXIMATE)

1 square inch (sq in, in^2) = 6.5 square centimeters (cm^2)

1 square foot (sq ft, ft^2) = 0.09 square meter (m^2)

1 square yard (sq yd, yd^2) = 0.8 square meter (m^2)

1 square mile (sq mi, mi^2) = 2.6 square kilometers (km^2)

1 acre = 0.4 hectare (he) = 4,000 square meters (m^2)

MASS - WEIGHT (APPROXIMATE)

1 ounce (oz) = 28 grams (gm)

1 pound (lb) = 0.45 kilogram (kg)

1 short ton = 2,000 pounds (lb) = 0.9 tonne (t)

VOLUME (APPROXIMATE)

1 teaspoon (tsp) = 5 milliliters (ml)

1 tablespoon (tbsp) = 15 milliliters (ml)

1 fluid ounce (fl oz) = 30 milliliters (ml)

1 cup (c) = 0.24 liter (l)

1 pint (pt) = 0.47 liter (l)

1 quart (qt) = 0.96 liter (l)

1 gallon (gal) = 3.8 liters (l)

1 cubic foot (cu ft, ft^3) = 0.03 cubic meter (m^3)

1 cubic yard (cu yd, yd^3) = 0.76 cubic meter (m^3)

TEMPERATURE (EXACT)

$[(x-32)(5/9)]$ °F = y °C

METRIC TO ENGLISH

LENGTH (APPROXIMATE)

1 millimeter (mm) = 0.04 inch (in)

1 centimeter (cm) = 0.4 inch (in)

1 meter (m) = 3.3 feet (ft)

1 meter (m) = 1.1 yards (yd)

1 kilometer (km) = 0.6 mile (mi)

AREA (APPROXIMATE)

1 square centimeter (cm^2) = 0.16 square inch (sq in, in^2)

1 square meter (m^2) = 1.2 square yards (sq yd, yd^2)

1 square kilometer (km^2) = 0.4 square mile (sq mi, mi^2)

10,000 square meters (m^2) = 1 hectare (ha) = 2.5 acres

MASS - WEIGHT (APPROXIMATE)

1 gram (gm) = 0.036 ounce (oz)

1 kilogram (kg) = 2.2 pounds (lb)

1 tonne (t) = 1,000 kilograms (kg)

= 1.1 short tons

VOLUME (APPROXIMATE)

1 milliliter (ml) = 0.03 fluid ounce (fl oz)

1 liter (l) = 2.1 pints (pt)

1 liter (l) = 1.06 quarts (qt)

1 liter (l) = 0.26 gallon (gal)

1 cubic meter (m^3) = 36 cubic feet (cu ft, ft^3)

1 cubic meter (m^3) = 1.3 cubic yards (cu yd, yd^3)

TEMPERATURE (EXACT)

$[(9/5) y + 32]$ °C = x °F

QUICK INCH - CENTIMETER LENGTH CONVERSION

Inches: 0 1 2 3 4 5

Centimeters: 0 1 2 3 4 5 6 7 8 9 10 11 12 13

QUICK FAHRENHEIT - CELSIUS TEMPERATURE CONVERSION

°F -40° -22° -4° 14° 32° 50° 68° 86° 104° 122° 140° 158° 176° 194° 212°

°C -40° -30° -20° -10° 0° 10° 20° 30° 40° 50° 60° 70° 80° 90° 100°

For more exact and or other conversion factors, see NIST Miscellaneous Publication 286, Units of Weights and Measures. Price $2.50 SD Catalog No. C13 10286

Updated 6/17/98

iv

TABLE OF CONTENTS

TABLE OF CONTENTS (cont.)

TABLE OF CONTENTS (cont.)

LIST OF FIGURES

LIST OF TABLES

LIST OF TABLES (cont.)

1. INTRODUCTION

This report presents the third in a series of studies[1,2] based on wake vortex data collected at various airports from 1975 through 1980. The measurements from these data collection efforts are now incorporated into a set of databases which can be used to answer questions about wake vortex behavior. The ultimate goal of these studies is to improve airport capacity by adopting operational procedures that more accurately reflect wake vortex behavior.

Two wake-vortex sensors, the Ground-Wind Vortex Sensing System (GWVSS) and the Monostatic Acoustic Vortex Sensing System (MAVSS) were used to collect most of the available wake-vortex data. The GWVSS was used more extensively and has the capability of tracking stalled wake vortices, such as might pose a hazard to a following aircraft on the same runway. On the other hand, although the MAVSS cannot detect stalled vortices, it has the advantage of measuring vortex strength. Since it can readily detect moving vortices, it is useful for studying wake vortices that move from one runway to a parallel runway.

The analysis of wake vortices stalled near the runway centerline was the primary goal of wake-vortex studies[3,4,5] before 1984. However, in 1984 the Volpe Center completed two draft studies of vortex lateral transport which pertain to the wake-vortex hazard for closely-spaced parallel runways. Current separation standards require that parallel runways separated by less than 2500 feet must be considered a single runway for wake-vortex purposes.

The first 1984 study[1] used GWVSS data alone to analyze the probability of wake vortices reaching a parallel runway. A transport model was developed to relate the wake-vortex hazard probability for a parallel runway to that for a single runway. This relationship was then used to extend the single-runway separation standards, which are established as safe from 15 years experience, to parallel runways. The results of this study indicated that the parallel-runway separation standard might be substantially less than 2500 feet for some classes of aircraft. The major deficiency of this study was an invalid assumption about the GWVSS, namely that the wake-vortex detection threshold does not depend upon the crosswind.

The second 1984 study[2] analyzed the MAVSS collected concurrently with the GWVSS data during the O'Hare departure data collection effort. A comparison of MAVSS and GWVSS data showed that the GWVSS fails to detect many vortices which are indicated as hazardous by the MAVSS. The loss of GWVSS sensitivity for laterally moving vortices may be related to two effects, the masking of the vortex signals by the crosswind and/or the reduction in signal strength as the vortex height above the ground increases. In either case, the GWVSS data underestimate the wake-vortex lateral transport probability and hence are questionable for assessing wake-vortex safety with respect to vortex decay for parallel runways. Consequently, MAVSS data should be used for parallel runway vortex decay studies.

Note that, under visual flight rules (VFR), aircraft typically use side-by-side approaches to close-spaced parallel runways. Currently, efforts are underway to enable such approaches under some conditions requiring instrument flight rules (IFR). Since the wake-vortex safety of side-by-side approaches depends upon vortex transport over relatively short times (e.g., less than 50 seconds), the GWVSS may be adequate for assessing wake-vortex safety at low altitudes, since vortex decay is not a major factor for large aircraft in this time frame.

1.1 PURPOSE OF STUDY

The present study extends the analysis of the two earlier studies to examine how the crosswind affects lateral vortex transport. This analysis will elucidate the differences between the GWVSS and MAVSS data and may assist in developing an improved lateral transport model that can validate parallel runway separation standards. In addition, the analysis provides additional information about algorithms for a parallel runway dynamic spacing system, such has been under development[6] in Germany since the mid 1980s. For example, simultaneous, dependent operations on close-spaced parallel runways may be permitted when the larger aircraft are assigned to the downwind runway. Basic questions for such a system are (a) how much crosswind is needed to assure safety and (b) how well the required crosswinds can be predicted.

1.2 DATABASE DEVELOPMENT

The first analyses of the 1975-1980 wake vortex data were based on *ad hoc* minicomputer databases. In 1984, the O'Hare landing and takeoff wake vortex and meteorological data were incorporated into the "flat" databases of the Statistical Analysis System (SAS), which were installed on the mainframe computers of the National Institute of Health. The original analyses for this report were conducted using SAS. The SAS databases were returned to the Volpe Center on magnetic tape.

The flat format of the SAS databases is inconvenient since each potential parameter for each run must have its own field. The O'Hare takeoff database had more than 300 fields, many of which are empty for each departure. Changing to a relational database structure permits a consolidation of parameters into a subordinate database containing multiple entries for each run. Such a format is particularly appropriate for MAVSS data, where as many as 10 detections can occur for each of the two vortices. In 1993, the flat SAS databases were converted into Paradox relational databases (Appendices B and C present the formats for landing and takeoff, respectively).

The plots from the original SAS analysis were generated as line-printer plots or CalComp plotter hard copies. Since these formats are not suitable for current reports, the plots were regenerated using a simplified Paradox database analysis and/or the plotting capabilities of Excel. The results were compared to the original SAS plots to detect any significant variations from the first analyses.

1.3 SCOPE

The distance that a vortex will travel laterally from a generating aircraft depends on many factors (its initial strength and the prevailing meteorological conditions, for example). The most significant factor is the ambient crosswind. This study examines the probability of vortex transport under different crosswind conditions. The basic question to be answered is what lateral distance a vortex can travel (under favorable or adverse wind conditions) while remaining potentially hazardous to an encountering aircraft. The primary analysis uses the O'Hare landing and takeoff MAVSS databases. In some cases, the takeoff GWVSS data are shown for comparison. Note that the landing GWVSS database is not useful for parallel runways since the anemometers extended only 350 feet from the extended runway centerline.

2

Chapter 2 describes the two vortex sensing systems used in this study, the organization of the vortex data into easily accessible datasets, and the analytical methods used to determine the various probability estimates. In addition, this section describes the results of a consistency check of vortex detections across the two sensing systems using the O'Hare takeoff data. Chapter 3 discusses of the different probability plots generated from the analysis, in particular the dependency of vortex transport on crosswind. Chapter 4 examines the influence of ground proximity on vortex behavior. Chapter 5 evaluates the characteristics of takeoff wake vortices that have traveled laterally a long distance (400 m). Chapter 6 summarizes the results of Chapters 3 through 5. Chapter 7 presents current considerations and recommendations.

In general, the analysis in this report represents the understanding of wake behavior in the mid 1980s. Much of the information in the O'Hare landing and takeoff databases relevant to parallel runway operations is evaluated within that context. Although the results may not be directly applicable to current parallel runway questions because of test, data reduction, or analysis limitations, they demonstrate analysis methods that may be adapted to the analysis of new datasets or the reanalysis of the O'Hare datasets.

1.4 SUMMARY OF FINDINGS

Results of this analysis show that, at a lateral distance of 400 m from an aircraft that is taking off, the only potentially hazardous vortices were those that were blown across by a favorable crosswind (i.e., one blowing in the direction that the vortex traveled). No vortices were observed to travel this distance against an adverse crosswind. The MAVSS detected more vortices at this distance than did the GWVSS, possibly because such vortices traveled out with higher crosswinds, and the GWVSS is not so reliable under high crosswind conditions. As expected, the vortex transport probability was observed to depend on the crosswind, generally increasing with favorable crosswind speed.

This page intentionally blank

2. DATABASES

2.1 DATA COLLECTION

Table 1 summarizes the O'Hare data collection efforts which generated the data to be used in this study. The landing[4,7,8] and takeoff[2] data were collected during two separate periods under different conditions, on different runways, and with somewhat different meteorological sensors.

Table 1. Data Collection at Chicago's O'Hare Airport

	LANDING		TAKEOFF
Dates	7/76-9/77		2/80-10/80
Runways	32L	14R	22L
MAVSS Runs Recorded	8715	8163	8836
MAVSS Locations (m)*	-305 to 122	-244 to 122	-244 to 396
Distance (m) from Runway	Threshold: 655	Threshold: 503	End: 2103
GWVSS Locations (m)*	-107 to 107	-107 to 107	-244 to 549
Distance (m) from Runway	Threshold: 472	Threshold: 472	End: 2103

*With respect to extended runway centerline

2.2 SENSORS

Two sensing systems were deployed, the Monostatic Acoustic Vortex Sensing System (MAVSS) and the Ground-Wind Vortex Sensing System (GWVSS). Since these systems are discussed in prior reports, summary descriptions are presented in Appendix A.

The spatial coordinate system used in the analysis is defined from the pilot's view-point. Assuming the aircraft is taking off or landing on the runway centerline, distances on the pilot's right (starboard side) are defined as positive, while those on his left (port side) are defined as negative. The sensor lines (GWVSS and MAVSS) stretch laterally across the pilot's field of view and are perpendicular to the runway centerline. Table 2 lists the sensor locations for the two tests.

2.3 DATABASE GENERATION

The data collected at O'Hare consisted of GWVSS, MAVSS, and meteorological measurements; aircraft information; and photographs of the aircraft path (takeoff only). The data reduction process produced wake vortex information from the vortex sensors (e.g., vortex strength, height, and lateral position as a function of vortex age from the MAVSS) and meteorological information (e.g., headwind, crosswind, temperature, etc.) at the time of the vortex measurements. The primary identification tag for the data was the arrival time of the aircraft.

2.3.1 SAS Databases

Because the raw data for different sensors were recorded on separate magnetic tapes, the data reduction process resulted in separate databases for each type of data. The studies prior to 1984 used *ad hoc* database systems set up on minicomputers. For the 1980s studies the databases were transferred to the Statistical Analysis System (SAS) operating on a mainframe computer. The separate databases were merged so that all the information collected for a given aircraft run was immediately accessible in one large data record. Records for landing aircraft were put into one database, and those

5

for takeoff into another. Two separate databases were used because landing and takeoff operations differ considerably (for example, there were no aircraft height data taken for landings) and they may yield different vortex behavior.

Central to the analysis of this report is the calculation of the probability that a vortex will travel a certain distance under a certain crosswind condition. For reliable calculations, the data must exhibit a high degree of accuracy and consistency. Although the processed data obtained from the original data reduction was extensively edited, nevertheless, certain inconsistencies remained. The following inconsistencies were flagged and runs containing them were excluded from the SAS analysis:

1. A vortex having a transport speed of more than 10 meters per second (either unrealistic or poor data quality).

2. A vortex moving in towards the runway centerline (vortices usually move out from the centerline).

3. A vortex detected on both sides of the runway centerline (unrealistic as the MAVSS only detects vortices far from the centerline; a vortex detected on one side would not be able to move the long distance required to be detected on the other side).

4. Both vortices from an aircraft detected on the opposite side of the centerline from where they were generated (unrealistic); that is, the port and starboard vortices were interchanged.

5. The two sensing systems disagreeing as to which direction from the centerline a given vortex traveled.

Table 2. Sensor Locations (ft) at O'Hare (with respect to extended runway centerline)

TAKEOFF		LANDING		
MAVSS	GWVSS	MAVSS		GWVSS
	Line 2	32L	14R	
		-1000		
-800	-800	-800	-800	
	-700			
-600	-600	-600	-600	
	-500			
	-450			
-400	-400	-400	-400	
	-350			-350
	-300			-300
	-250			-250
-200	-200	-200	-200	-200
	-165			-150
				-100
				-50
				0
				50
				100
	165			150
200	200	200	200	200
	250			250
300	300			300
	350			350
	400	400	400	
	450			
	480			
	730			
750	760			
	800			
900	900			
	1000			
1100	1100			
	1200			
1300	1300			
	1400			
	1500			
	1600			
	1700			
	1800			

6

2.3.2 Paradox Databases

In 1993, the SAS databases used in the 1980s analyses were converted into Paradox relational databases, which were used for all the new analyses presented in this report. The quality checks described in the last section were not repeated for the Paradox analyses. Some may have been used, however, to remove invalid parameters from the SAS database before it was returned to the Volpe Center for subsequent conversion to Paradox. In general, the Paradox analyses differed from the SAS analyses by only a small number of cases; the intensive effort needed to repeat the validations was deemed not cost effective.

The relational databases, described in Appendices B and C for landing and takeoff, respectively, include four components:

1. Run data (date/time, aircraft type, etc.),

2. Meteorological data,

3. GWVSS data, and

4. MAVSS detection data

Strictly speaking, only the MAVSS detection database is truly relational, with many records for each run. The meteorological and GWVSS databases have only one record for each run. The separation of the meteorological and GWVSS data is for convenience, not relational logic.

2.4 DATABASE CHARACTERISTICS

2.4.1 Aircraft Types

Table 3 lists the aircraft types for the three databases useful for parallel runway studies. The MAVSS numbers for landing differ considerably from the numbers in Table 1 for the SAS databases since Table 3 lists only MAVSS runs processed. After a certain point in the processing of landing data, the common aircraft types (e.g., B-727) were no longer processed. Also, a smaller fraction of Runway 14R MAVSS runs were processed since the 14R 305-m antenna was usually not functioning. The B-727, DC-9 and DC-10 have the largest number of runs and will be used for the analyses of this report. They represent three different aircraft sizes.

The number of runs having MAVSS detections are also listed in Table 3 for the MAVSS. Vortices were detected for most of the landing runs, where all aircraft follow the same flight path. Fewer vortices were detected for takeoff, presumably because of the variability in aircraft flight path.

7

Table 3. Distribution of Aircraft Types

Type	LANDING MAVSS RUNS Processed	With Data 32L	With Data 14R	TAKEOFF MAVSS Processed	With Data	RUNS GWVSS
Unknown	1	0	0	1	1	784
707	678	461	185	227	133	405
707 H	95	75	17	237	134	372
727	2,567	1944	470	4308	2769	7697
737	341	262	42	639	362	1288
747	273	170	100	163	97	277
A-300	0	0	0	1	0	5
DC-10	562	333	215	883	735	1377
DC-8	280	162	109	11	10	22
DC-8 H	145	73	67	253	188	414
DC-9	1,238	903	192	1436	754	2720
KC-135	0	0	0	20	15	27
L1011	174	126	42	178	155	287
LG PROP	47	36	1	113	44	263
OTHER	0	0	0	1	1	2
SM JET	103	38	6	96	22	205
SM PROP	505	148	56	193	18	643
VC-10	3	2	0	0	0	0
TOTAL	7,011	4731	1502	8760	5438	16788

2.4.2 MAVSS Detections

The quality of the MAVSS data depends upon the number of vortex detections. At least two detections are required to obtain an accurate transport speed, which is needed for accurate circulation measurements. Tables 4 and 5 show the number of MAVSS detections (N) for the vortices generated (two per run) by common jet transport aircraft for landing and takeoff, respectively.

For landing (Table 4), the number of vortices with more than two detections drops rapidly since one side of the runway was instrumented with only two antennas.

For takeoff (Table 5), a similar drop is noted above four detections, since only four antennas are located on one side of the runway. The fraction of vortices with no detections is greater for takeoff than landing, for the reasons noted above.

8

Table 4. Number of MAVSS Detections for Landing
Vortices (Both Port & Starboard), by Aircraft Type

Type	N=0	N=1	N=2	N=3	N=4	N=5	TOTAL
707	199	322	530	135	160	10	1356
707 H	23	35	101	12	19	0	190
727	1019	1413	1892	462	329	19	5134
737	152	214	242	41	32	1	682
747	77	104	202	64	95	4	546
DC-10	140	219	421	160	173	11	1124
DC-8	83	102	216	66	89	4	560
DC-8 H	33	60	106	43	48	0	290
DC-9	620	733	861	152	105	5	2476
L1011	53	64	147	30	49	5	348

Table 5. Number of MAVSS Detections for Takeoff
Vortices, by Aircraft Type

Type	N=0	N=1	N=2	N=3	N=4	N=5	N=6	TOTAL
707	235	75	79	30	23	9	3	454
707 H	247	71	86	44	14	8	4	474
727	4511	1486	1752	542	224	71	28	8614
737	703	210	268	64	30	3	0	1278
747	174	51	38	23	28	8	4	326
DC-10	653	279	367	213	142	68	44	1766
DC-8	5	3	6	7	1	0	0	22
DC-8 H	209	67	123	51	38	12	6	506
DC-9	1670	475	512	150	48	13	4	2872
L1011	99	57	89	47	40	14	10	356

2.4.3 Crosswind Distribution

Figure 1 shows the crosswind distribution for arrivals on the three runways where GWVSS systems
were installed. Runways 14R and 32L have asymmetric crosswind distributions, favoring winds from
the southwest. This crosswind direction blows toward the short end of the MAVSS baseline for 32L
and the long end of the MAVSS baseline for 14R. Unfortunately, the last antenna on the long end of
14R was often out of service.

Figure 2 shows the crosswind distribution for departures. It is close to symmetric, with only a slight
bias toward positive crosswinds, the longer end of both the MAVSS and GWVSS baselines.

The O'Hare 50-foot wind towers were part of the Vortex Advisory System installation[4]. The
measurement locations were somewhat removed from the GWVSS and MAVSS locations, roughly
500 m for 500 m for all three runways.

9
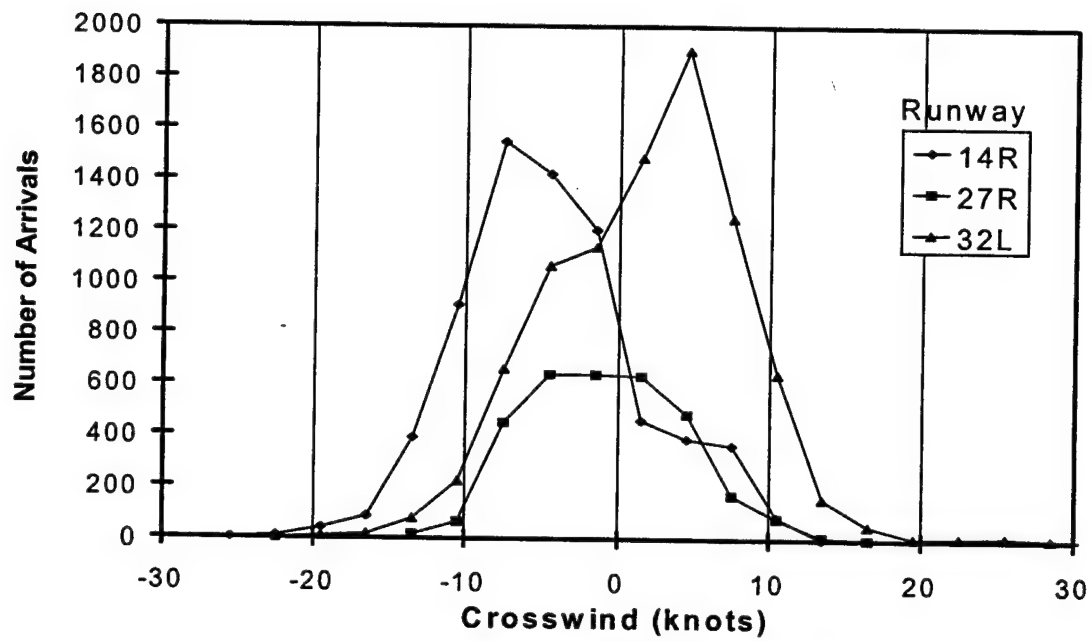
Figure 1. Crosswind Distribution for Arrivals
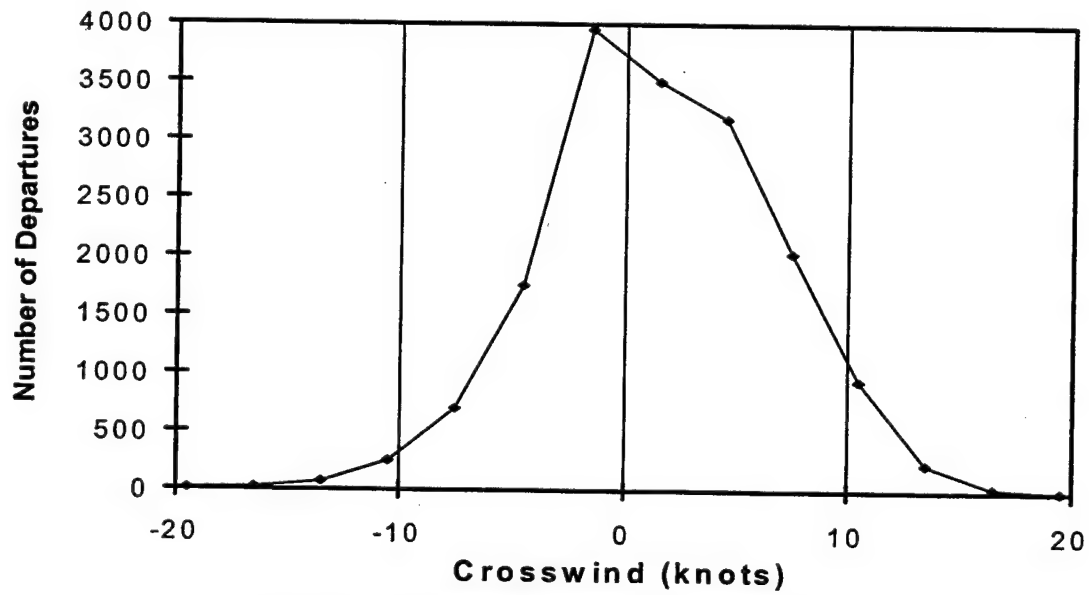
Figure 2. Crosswind Distribution for Departures

3. ANALYSIS OF TRANSPORT PROBABILITY

3.1 METHODOLOGY

In this analysis of vortex transport probabilities, the "detection" of wake vortices is used to generate the desired probabilities. This approach allows the MAVSS and GWVSS data to be compared on an equal basis. MAVSS strength measurements will be considered in Chapter 5.

Previous studies involved with separation standards for parallel runways looked at those cases where vortices traveled the farthest. This study is concerned with finding the crosswind conditions under which vortices will not be transported a certain distance, viz., the distance to a parallel runway. With knowledge of the wind conditions that preclude vortex transport to a parallel runway, one could potentially decide - based upon current crosswind conditions - whether a pair of runways could be operated simultaneously without being subject to wake vortex safety constraints.

The analysis will estimate the probability that a vortex will travel a certain distance under a given crosswind condition, i.e., for measured crosswinds within certain limits. The conditional probability is estimated as:

$$P = m/n \qquad (1)$$

where:

P = the probability that a vortex gets to the sensor at a distance X from the centerline,

m = the number of vortices detected at (or beyond for SAS analysis) that sensor, and

n = the total number of vortices generated under the given crosswind limits (two vortices per run).

This definition of the transport probability differs somewhat from that used in References 1 and 2 where all crosswinds were included and the value of n was taken as the number of vortices that traveled toward a certain side of the runway. The procedure used in this report is better defined; in the previous studies it was difficult to assign the direction of travel for wake vortices that were not detected by the sensors.

To properly interpret the results obtained from Equation 1, it is useful to examine the statistical accuracy of the estimate obtained from the experimental data. In the nomenclature of statistics this type of data is known as a binomial distribution. An experiment is performed n times with two possible outcomes, vortex detected or vortex not detected (at a particular distance), with an assumed constant probability of the results for each trial. For a particular set of trials, the number of vortex detections is m. The basic question to be answered is how accurate is the value of probability given by Equation 1. The accuracy can be stated in terms of the standard deviation σ of the probability P which is obtained from statistical analysis as:

$$\sigma = [P(1-P)/n]^{1/2}. \qquad (2)$$

11

For small probabilities this result can be approximated by:

$$\sigma = [P/n]^{1/2} = m^{1/2}/n. \qquad (3)$$

Another useful expression is the fractional standard deviation given by:

$$\sigma/P = 1/m^{1/2}. \qquad (4)$$

For the probability measurement to have statistical significance, the fractional standard deviation must be much less than one, i.e., the statistical error must be less than the value measured. Thus, according to Equation 4, a meaningful probability measurement requires m to be perhaps at least 10 (fractional standard deviation of 0.32). The lowest possible nonzero estimate of probability is 1/n (m=1) where the fractional standard deviation is 1.0. Thus, for confidence in the measurement the measured probability must be perhaps 10 times above the value 1/n. The probability 1/n will be included on the data plots to give an indication of measurement reliability.

Some restrictions were placed on which data records were used to calculate the transport probabilities. First, the height of the aircraft in any run used in the analysis had to be above 0 m (i.e., airborne) and below 107 m (within sensor range) at the time it crossed the sensor line. This restriction applied only to the takeoff database, as the landing database did not have aircraft height information (landing heights were expected to be about 50 m). Second, runs lacking critical data, such as headwind or crosswind, were not used. Third, when an analysis involved the use of MAVSS data, inconsistent records (Section 2.3) were eliminated explicitly from the original SAS analysis, but not from the plots of this report. In addition, for the landing analysis, a special correction was made for data recorded by the MAVSS sensor at -305 m from the centerline. This sensor was operational reliably on only one of the two runways used, namely runway 32L. Therefore, the denominators used in calculating the vortex transport probabilities at -305 m had to be reduced to include only those runs landing on runway 32L.

The study concentrated on vortices generated by the following aircraft types: DC-10, DC-9, and B-727, as these occurred most frequently at O'Hare airport. For statistical purposes, the large number of measurements of vortices generated by these aircraft types provided a more reliable basis for probability estimation.

3.2 WIND DEPENDENCE

3.2.1 MAVSS

Figure 3 shows the effect of crosswind on the probability of a vortex reaching a certain distance for the three aircraft types, using MAVSS takeoff data. The numbers on the x-axis are the mid-points of crosswind bins used in the analysis, which were increments of 3 knots. Bins were included in the analysis only if the number of runs was greater than ten. A negative crosswind is one blowing toward the negative side (to the pilot's left). Thus, the point at 1.5 knots on the x-axis references all crosswinds between 0 and 3 knots. The numbers on the y-axis are the probabilities of vortex transport for a given crosswind range. This axis has a logarithmic scale. The numbers on the axis are the actual probability values (the value of zero cannot, of course, be represented on a logarithmic scale). A particular line in Figure 3 (for example, the one labeled '+61 m') shows how the probability of a vortex (from a DC-10 aircraft taking off for the top plot) reaching the sensor at +61 m on the positive side of

the runway, will change as crosswind conditions vary from -15 to +15 knots. The probability is very low for crosswinds below -5 knots, reaches 20 percent probability for zero crosswind and levels off at about 60 percent probability for crosswinds above +5 knots. Note that, for the antenna at +91 m, the probability rises to a higher asymptotic limit (roughly 90 percent at +10-knot crosswind). For large positive crosswinds the detection probability at +61 m is reduced because the vortex arrives so quickly that its MAVSS signature is obscured by aircraft noise.

The lines of Figure 3 are identified in two ways:

1. Solid lines are used for negative lateral positions and dotted lines for positive lateral positions.

2. The same plotting symbol is used for similar distances on either side of the runway.

The dashed line across the lower part of each plot is used to assess the confidence associated with specific points. It represents the reciprocal of the number of data samples for each crosswind range. (See the discussion of Equations 1-4 above.) Greater confidence can be placed in measurements farther above the dotted line. The selection of crosswind increments of 3 knots gives an adequate number of data samples while providing reasonable crosswind resolution.

Figure 4 shows crosswind analysis of MAVSS data for landing aircraft. In contrast to the roughly symmetrical takeoff data collection, the landing data collection deployed many more MAVSS antennas on the negative side of the runway (because of a parallel taxiway on the positive side).

If wake vortex behavior were the same on both sides of the runway, one would expect that the solid and dotted lines for the same plotting symbol (equivalent lateral distance on opposite sides of the runway) would be mirrored about zero crosswind. This expectation is reasonably well observed in Figures 3 and 4.

The landing plots of Figure 4 are virtually identical to the original SAS plots. The takeoff plots of Figure 3 have a number of one or two detection outliers that did not appear in the SAS plots, notably for the B-727. They can be observed as odd points just above the dashed limit line near the bottom of the B-727 (bottom) plot of Figure 3.

13
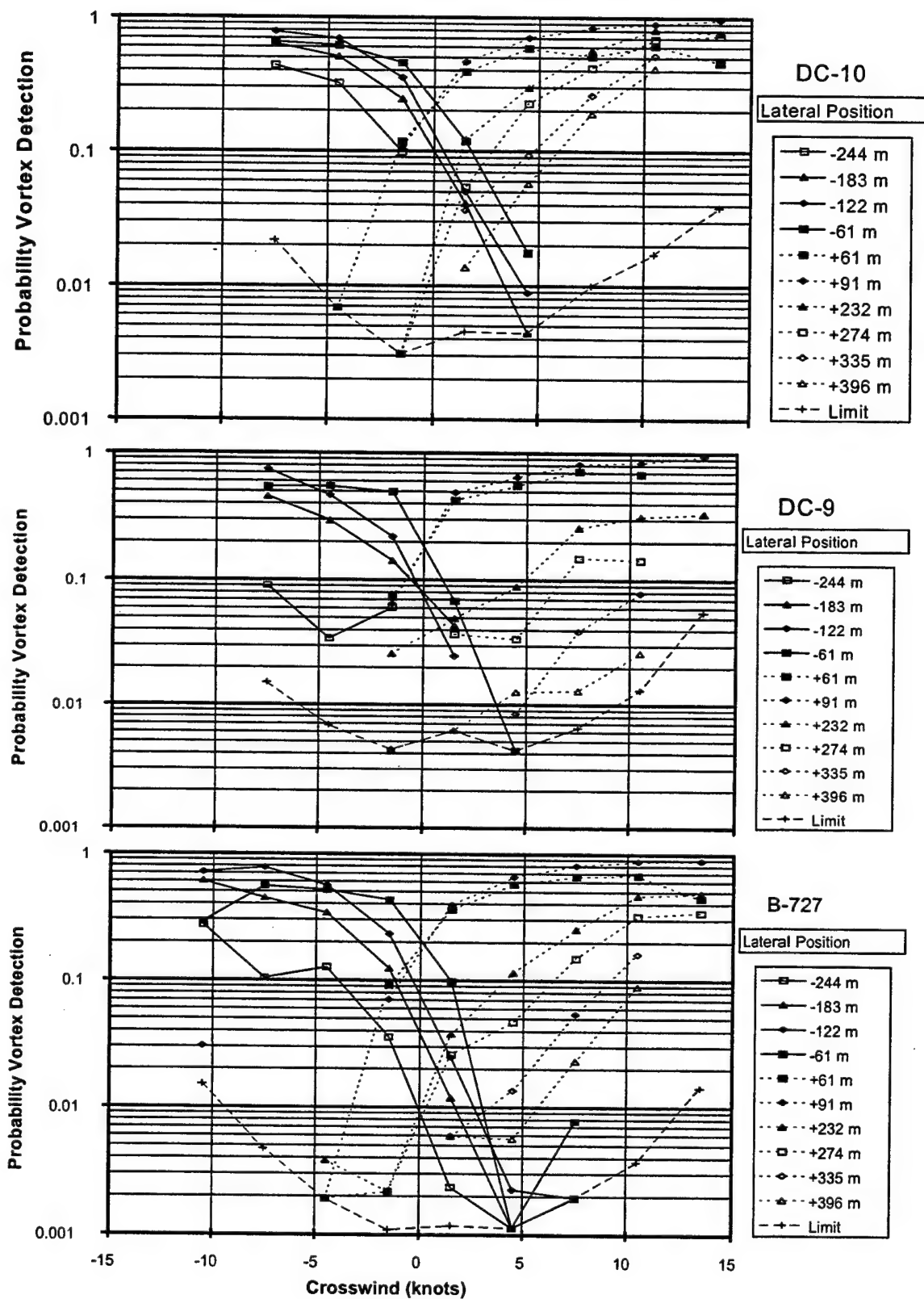
Figure 3. Dependence of MAVSS Takeoff Detection Probability on Crosswind

14
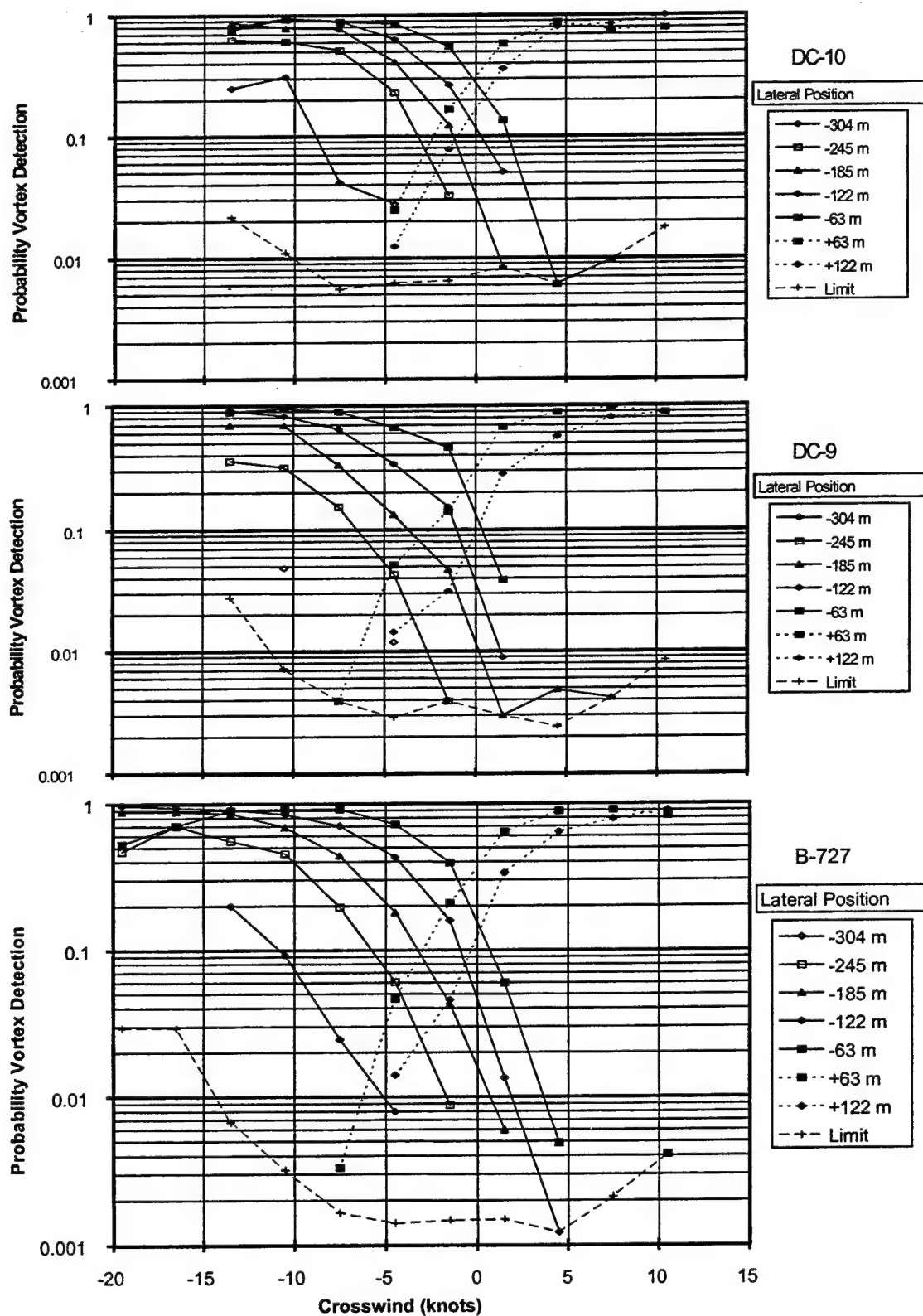
Figure 4. Dependence of MAVSS Landing Detection Probability on Crosswind

3.2.2 GWVSS

Figure 5 is similar to Figure 3 but shows GWVSS data instead of MAVSS. Note that the GWVSS generally gives a lower probability estimate than the MAVSS that vortices will reach a certain distance under given wind conditions. This difference will be more readily observed in the distance plots of the next section.

The GWVSS detection probability falls off more consistently (i.e., even for large lateral distances) with increased favorable crosswind than observed for MAVSS detection probability (note particularly negative crosswinds for the B-727, bottom of Figure 5). This decrease is likely related to the increased turbulence that accompanies larger crosswinds; the GWVSS sensitivity is reduced when the crosswind variance is increased.

3.3 DISTANCE DEPENDENCE

3.3.1 MAVSS

Figure 6 shows the MAVSS takeoff data of Figure 3 plotted in a different format. The x-axis plots the transport distance rather than the crosswind. Each line in Figure 6 indicates the probability of a vortex reaching various positive distances for a given crosswind range. Figure 7 plots the MAVSS landing data.

The scales in Figures 6 and 7 were selected to make the data lie approximately on a straight line. The x-axis has a distance (D) squared scale and the y-axis (probability P) has a logarithmic scale. A straight line on this plot indicates a functional dependence of transport probability (P) on transport distance (D) as:

$$P = a \exp(-bD^2) \qquad (5)$$

where a and b are constants. This functional dependence was observed in previous[1,2] analyses. Because the probability axis has a log scale, the smallest probability that can be plotted is that for a single vortex detection (1/n).

The lines in the plots are keyed by using solid lines for negative crosswinds and dotted lines for positive crosswinds. The same plotting symbols are used for positive and negative crosswinds of the same magnitude. Since both positive and negative distances are plotted on the same plot, two separate line segments appear for low crosswind magnitudes (e.g., 1.5 or 4.5 knots). The probability is lower when the crosswind and lateral distance have opposite signs, as would be expected.

Most of the plots show reasonable consistency for the probabilities for crosswinds of the same magnitude but opposite sign (i.e., the same plotting symbol). This consistency is expected if vortices transport similarly to the two sides of the runway.

16
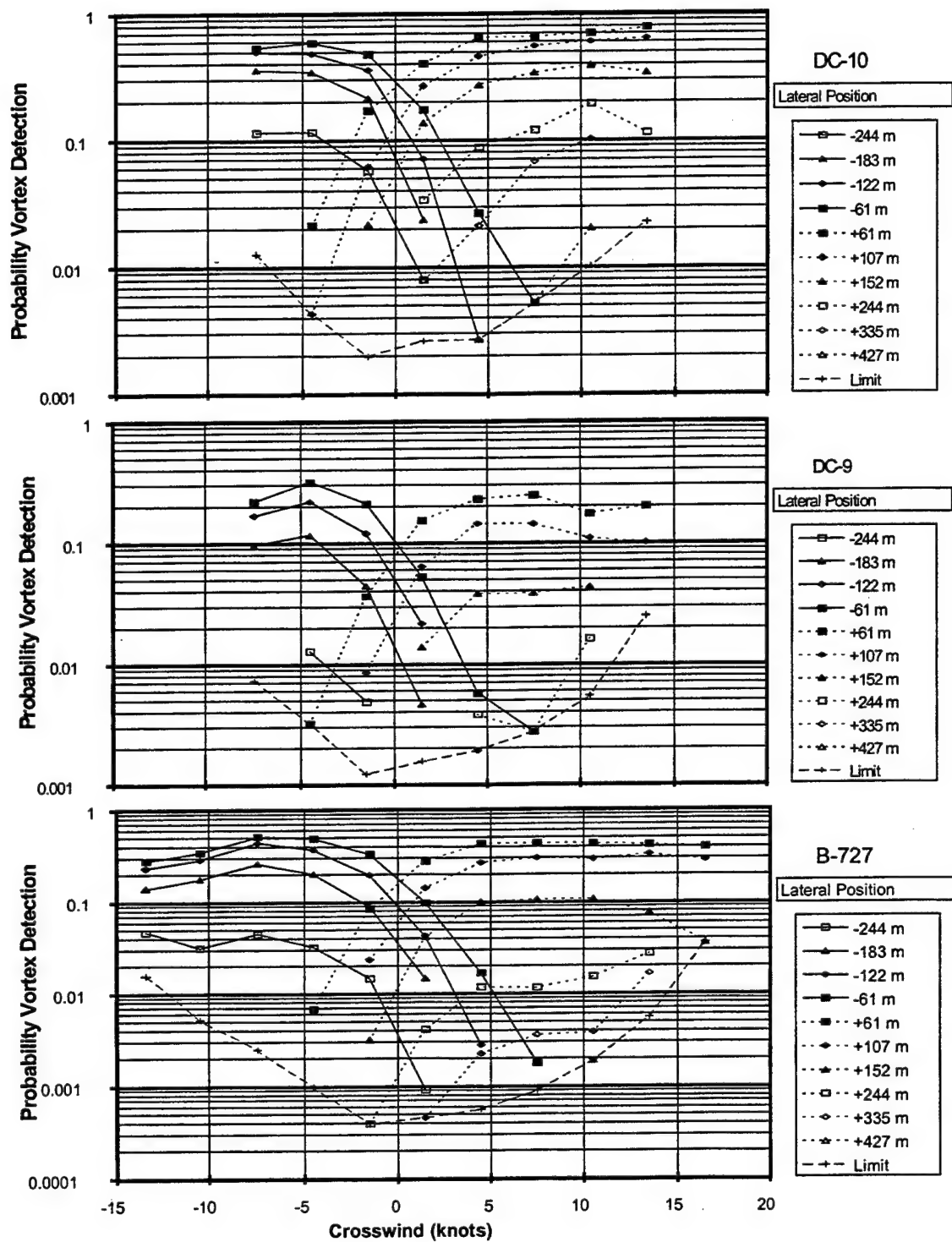
Figure 5. Dependence of GWVSS Takeoff Detection Probability on Crosswind
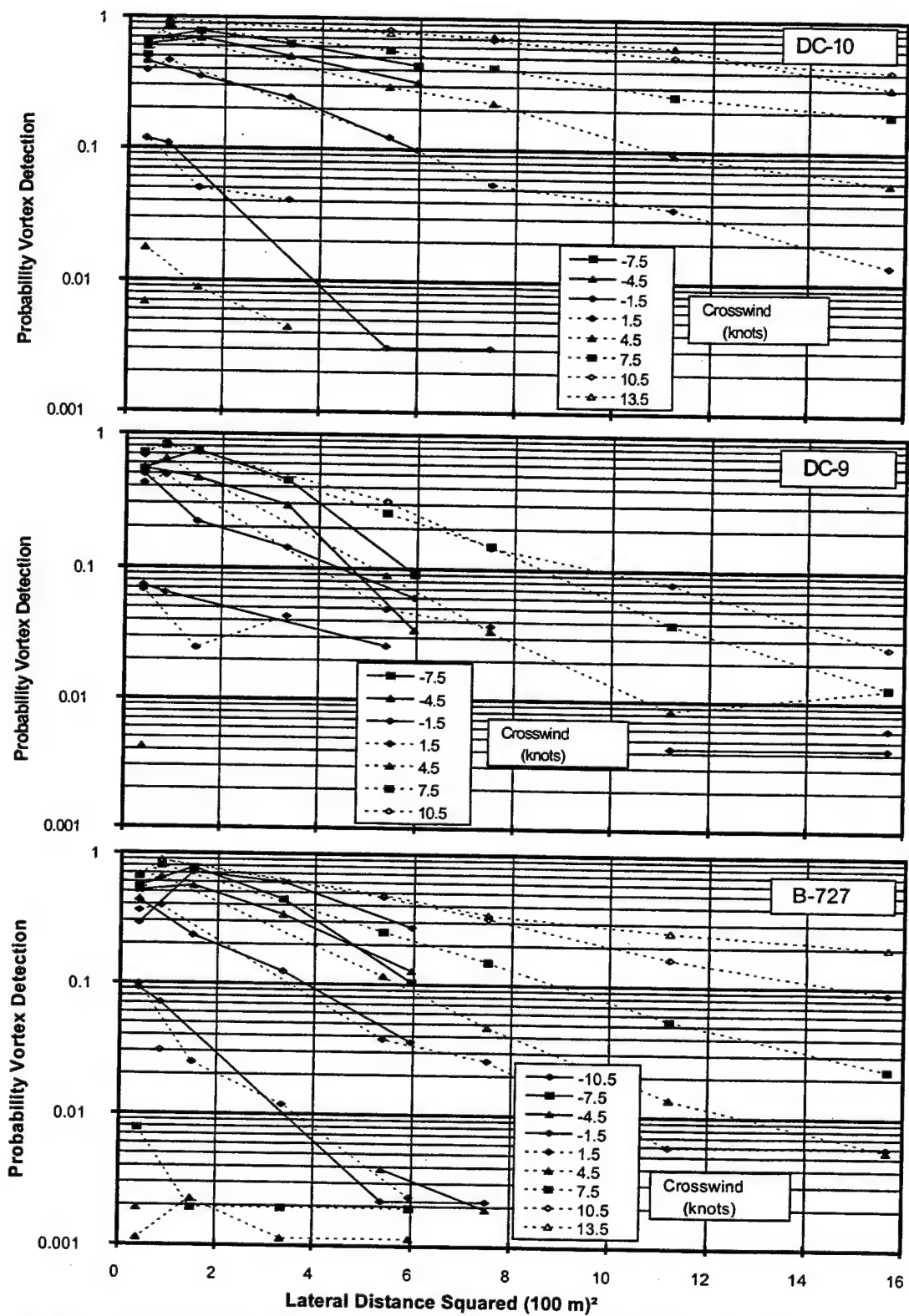
Figure 6. Dependence of MAVSS Takeoff Detection Probability on Lateral Distance Squared
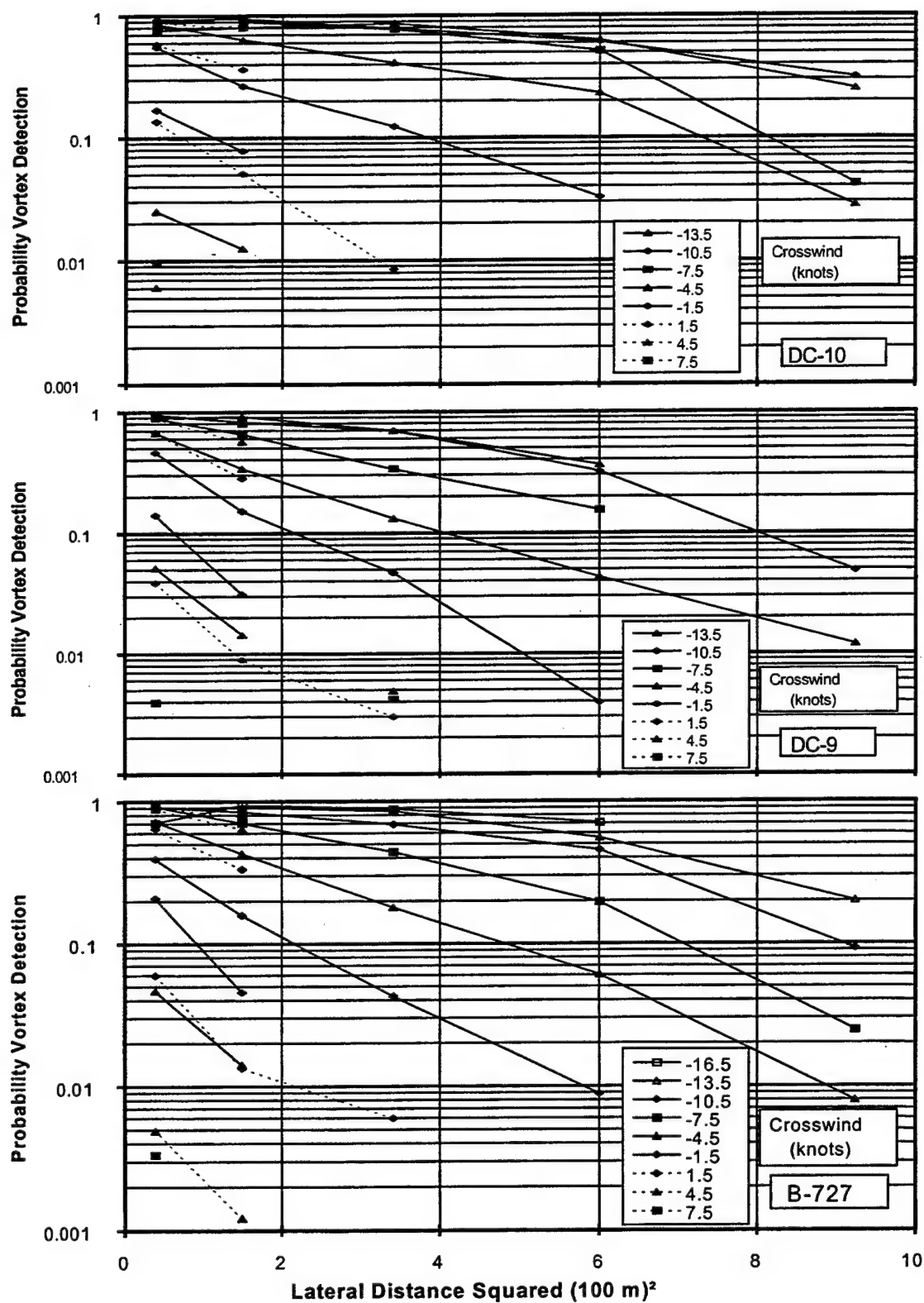
Figure 7. Dependence of MAVSS Landing Detection Probability on Lateral Distance Squared

19

3.3.2 GWVSS

Figure 8 plots the detection decay with distance for the GWVSS takeoff measurements. For the same crosswind, the decay is notably faster than for the MAVSS data in Figure 6.

The GWVSS results are not as consistent with crosswind direction as observed for both takeoff and landing MAVSS. In particular, the DC-9 and B-727 results in Figure 8 are significantly different for favorable crosswinds of opposite sign (e.g., 4.5 and 7.5 knots).

3.3.3 Comparisons

To facilitate comparisons between the three distance decay measurements (M - LA = MAVSS landing, M - TO = MAVSS takeoff, and G - TO = GWVSS takeoff), Table 6 presents the probability of reaching $(D/100)^2 = 5$ with a favorable crosswind of 4.5 knots. The log probabilities were averaged when data were available for two directions. The MAVSS takeoff and landing probabilities are comparable. The GWVSS takeoff probabilities are significantly lower.

Table 6. Probability of Reaching Lateral Position = 225 m with Crosswind of 4.5 Knots

	DC-9	B-727	DC-10
M - LA	0.07	0.09	0.3
M - TO	0.05	0.17	0.36
G - TO	0.015	0.035	0.15

3.4 SENSITIVITY TO SENSOR LIMITATIONS

Specific features of the two sensing systems affect the likelihood of detecting vortices under specific conditions. This section examines the impact of these features on data in the O'Hare takeoff database, and describes the consistency of the timing and location of apparent vortex detections at vortex death and at intermediate positions. The specific features include:

1. At times, only one side of the MAVSS line was activated: the side in the direction towards which the prevailing wind is blowing. This choice was made during playback to reduce the MAVSS processing time.

2. The vertical range of vortex detection for the GWVSS system is limited.

3. The detection threshold of the GWVSS system increases with greater ambient crosswind variations.

4. The horizontal range of MAVSS system is discrete. The MAVSS system can only detect vortices as they move directly across a MAVSS sensor. It is unable to track vortices between sensors.

5. The MAVSS correlator requires vortices to move at sufficient speed in order to detect them.

6. MAVSS detections may be lost due to the arrival of the next aircraft. Both MAVSS and GWVSS tracking is terminated with the arrival of the next aircraft. The GWVSS restriction is less serious; however, since the MAVSS is blanked by noise before the aircraft's arrival and also has a correlator width of 30 m which restricts how close to the end of a run MAVSS can detect a vortex. These limitations affect vortex detections at long times, i.e., for low crosswinds and large lateral transport distances.

20
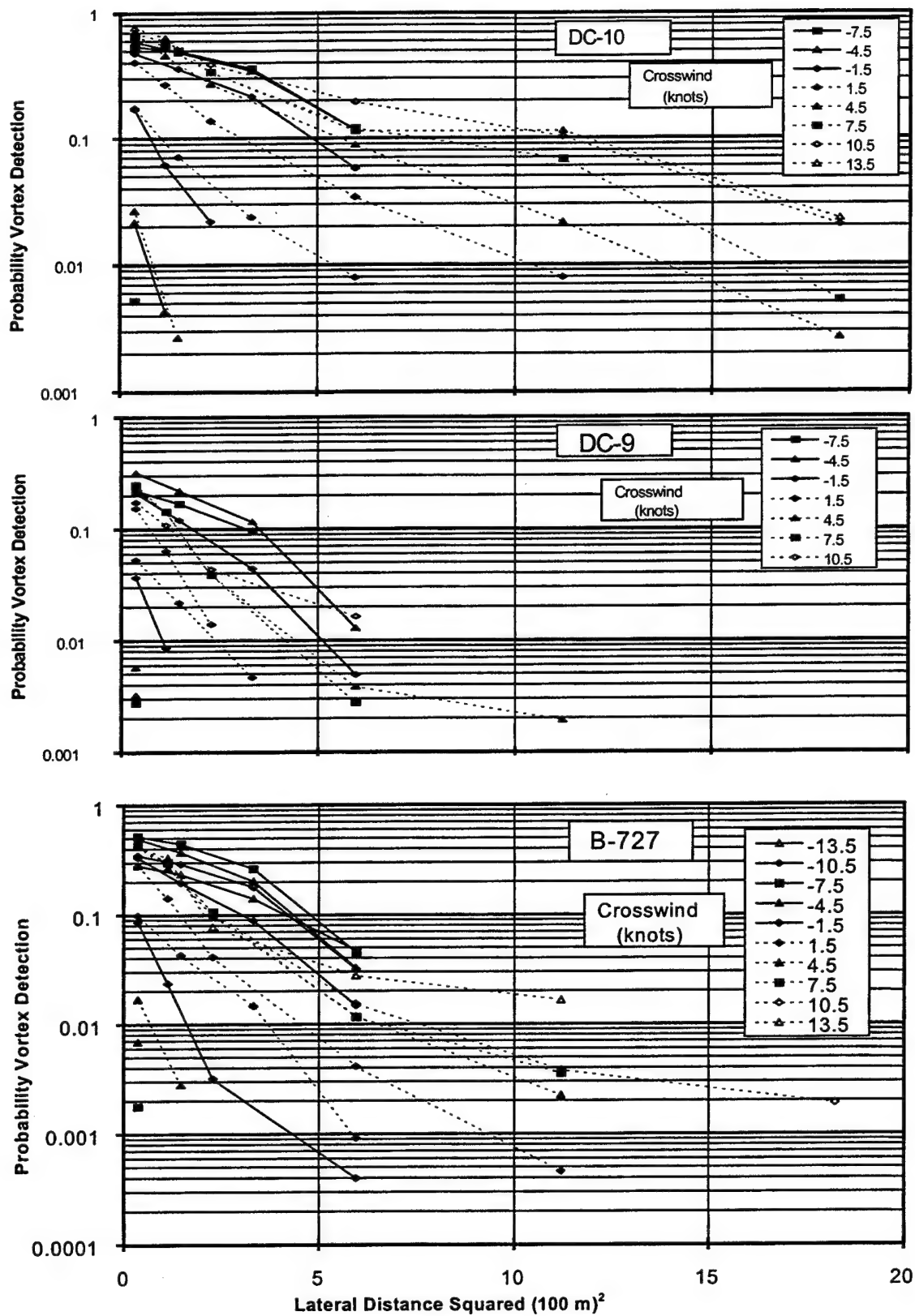
Figure 8. Dependence of GWVSS Takeoff Detection Probability on Lateral Distance Squared

3.4.1 MAVSS One-Side Processing

The following procedure was employed to determine the impact on the O'Hare takeoff database of using the prevailing wind conditions to determine whether or not to activate either or both sides of the MAVSS line. First, it was noted that the decision to

Table 7. Vortices Detected by GWVSS but Missed by MAVSS Because MAVSS Deactivated

Aircraft Type	MAVSS Detections	GWVSS Detections When MAVSS Deactivated
B-727	4345	6
B-747	163	0
DC-10	896	0

activate was made and remained in effect for an entire MAVSS tape (one or two days of MAVSS data collection). The MAVSS tape number corresponding to the original source of each observation in the takeoff database (Appendix C) is contained in the RUNTO field MTAPE. If all MAVSS observations for a given value of MTAPE were on one side of the line, and there were one or more GWVSS observations on the other side of the line, then the MAVSS were considered to be activated for one side of the line only. For observations with only one side of the MAVSS line activated, a count was made (Table 7) of the number of B-727, B-747, and DC-10 GWVSS detections on the de-activated side of the line, i.e., vortices that MAVSS could not detect because it was de-activated.

GWVSS detections when MAVSS was de-activated represent an insignificant proportion of the MAVSS detections. Thus, the decision to de-activate one side of the MAVSS line was appropriately made and will have little effect on the results of any analyses employing the takeoff database.

3.4.2 GWVSS Vertical Range Limit

The effect of the limited vertical range on GWVSS-based analyses was evaluated as follows. The probability of the GWVSS system ascribing the vortex death position at a distance equal to or greater than the last MAVSS detection was computed for various height ranges (Table 8). This probability declines with increasing vortex height. Thus, the restricted vertical range does have a significant impact on GWVSS-based analyses of the takeoff database. The effect is to reduce the apparent wake vortex transport hazard probability.

Table 8. Probability of GWVSS Death Position at a Distance Greater Than or Equal to the Last MAVSS Detection by Vortex Height

Vortex Height	Detections			GWVSS Probability		
	B-727	DC-10	B-747	B-727	DC-10	B-747
0-9 m	107	34	3	0.42	0.38	0.7
10-19 m	608	76	6	0.67	0.63	0.2
20-29 m	869	253	22	0.34	0.47	0.6
30-39 m	320	155	20	0.10	0.21	0.3
40-49 m	244	126	17	0.06	0.21	0.2
50-59 m	141	47	12	0.04	0.15	0.2
60-69 m	72	30	5	0.03	0.03	0.0
70-79 m	28	23	2	0.04	0.00	0.0
80-89 m	29	21	3	0.07	0.00	0.0
90-99 m	5	4	1	0.00	0.00	0.0

3.4.3 GWVSS Crosswind Variance

Crosswind variance affects the ground-wind detection threshold. The impact of changes in the crosswind threshold on GWVSS-based analyses was evaluated as follows. The crosswind variance is expected to be correlated to crosswind magnitude. Thus, crosswind magnitude and vortex transport

speed (which is correlated to crosswind magnitude) were used in this analysis as surrogates for crosswind variance. The probability of the GWVSS system ascribing the vortex death position at a distance equal to or greater than the last MAVSS detection was computed for vortex transport speed (Table 9) and crosswind (Table 10) ranges. The probability declines with increasing vortex velocity or crosswind; thus the impact on GWVSS-based analyses is significant. The effect is to reduce the apparent wake vortex transport probability.

Table 9. Probability of GWVSS Death Position at a Distance Greater Than or Equal to the Last MAVSS Detection by Vortex Transport Speed

Vortex Speed	Detections			GWVSS Probability		
	B-727	DC-10	B-747	B-727	DC-10	B-747
0-2 kts	704	276	47	0.44	0.48	0.40
3-5 kts	1365	395	40	0.33	0.26	0.20
6-8 kts	342	94	4	0.13	0.15	0.0
9-11 kts	12	4		0.0	0.0	

Table 10. Probability of GWVSS Death Position at a Distance Greater Than or Equal to the Last MAVSS Detection by Crosswind (CW) Speed

CW Speed	Detections			GWVSS Probability		
	B-727	DC-10	B-747	B-727	DC-10	B-747
0-2 kts	541	269	38	0.51	0.47	0.42
3-5 kts	877	281	30	0.33	0.27	0.30
6-8 kts	620	140	19	0.27	0.20	0.05
9-11 kts	294	57	4	0.19	0.23	0.3
12-14 kts	56	18		0.13	0.17	
15-17 kts	2	1		0.0	1.0	

3.4.4 MAVSS Discrete Locations and Transport Speed

The impact of vortex transport speed on the MAVSS detection threshold and, thus, on MAVSS-based analyses was observed as follows. The probability of the last MAVSS detection being at a distance greater than or equal to the GWVSS system vortex death position was computed for various vortex transport speed ranges (Table 11). Two algorithms were used:

1. Probability assumes MAVSS death position equals speaker distance of last detection.

2. Probability 1 assumes MAVSS death position equals distance of next antenna after last detection.

Table 11. Probability of MAVSS Death Position Equal to or Greater Than GWVSS Death Position by Vortex Transport Speed

Vortex Speed	Detections			MAVSS Probability			MAVSS Probability 1		
	B-727	DC-10	B-747	B-727	DC-10	B-747	B-727	DC-10	B-747
0-2 kts	704	276	47	0.56	0.52	0.60	0.98	0.97	0.91
3-5 kts	1365	392	40	0.67	0.75	0.80	0.98	0.97	0.95
6-8 kts	342	92	4	0.87	0.87	1.0	0.99	1.00	1.0
9-11 kts	12	4		1.0	1.0		1.0	1.0	

The higher vortex speed ranges have a somewhat higher probability, thus there appears to be some velocity effect on the MAVSS detection capacity. The effect is to reduce the apparent transport probability.

Several things should be noted of relevance to this last MAVSS detection threshold analysis:

1. For consistency, observations with GWVSS detections at distances beyond the last MAVSS antenna in the line were ignored in this analysis.

2. To obtain valid vortex velocities, only observations with at least two MAVSS detections were considered. Thus, this analysis is biased against slow moving vortices. In all likelihood, the effect is somewhat stronger than indicated.

An additional problem arises in this last analysis as follows. The MAVSS system does not yield a vortex death position. Assuming the vortex died at the point of its last detection is not valid. In fact, the vortex is likely to have died somewhere between the last vortex detection and the next MAVSS antenna farther from the runway centerline. Unfortunately, the MAVSS does not track the vortex between detections. Thus, the probability was recomputed as if the MAVSS system indicated a death at the next speaker beyond the speaker where the MAVSS last detected the vortex. The true probability is somewhere between the two probabilities computed in Table 11. The probabilities approach or equal 1 when computed assuming the vortex died at the following speaker. This effect is most likely due to the large gaps between MAVSS speakers (Table 2).

3.4.5 MAVSS Next Aircraft Arrival

MAVSS detections may be missed due to the arrival of the next aircraft. This problem was discussed in a previous[2] report. The GWVSS is less likely to miss detections due to the arrival of the next aircraft. Thus, aircraft inter-arrival times will affect the probability that the MAVSS death position was greater than or equal GWVSS death position. To estimate this impact the probabilities in Table 11 were recomputed eliminating observations in which an aircraft arrived within 10 seconds of the GWVSS death time (Table 12). As expected the probabilities increase. However, note that removing the inter-arrival effect does not eliminate the vortex transport speed effect, i.e., the probabilities in Table 12 still increase with increasing vortex speed.

Table 12. Probability of MAVSS Death Position Equal to or Greater Than GWVSS Death Position by Vortex Transport Speed - Corrected for Effect of Next Run

Vortex Speed	Detections			MAVSS Probability			MAVSS Probability 1		
	B-727	DC-10	B-747	B-727	DC-10	B-747	B-727	DC-10	B-747
0-2 kts	704	276	47	0.61	0.59	0.60	0.99	0.98	0.93
3-5 kts	1365	392	40	0.73	0.76	0.82	0.98	0.98	0.95
6-8 kts	342	92	4	0.90	0.87	1.0	0.99	1.00	1.0
9-11 kts	12	4		1.0	1.0		1.0	1.0	

3.4.6 GWVSS-MAVSS Detection Consistency

The consistency of GWVSS and MAVSS detections at intermediate locations was tested as follows. The takeoff database (Appendix C) includes vortex positions at 30, 60, 90, and 120 seconds. These GWVSS measurements are valid only when the vortex death time is greater than 30, 60, 90, and/or 120 seconds. Consider an intermediate GWVSS measurement at 30 seconds. It is compared with the MAVSS detection closest to 30 seconds. The MAVSS vortex position at 30 seconds is interpolated using the arrival time closest to 30 at a MAVSS speaker and the vortex velocity. The number and proportion of vortices which exhibit differences in apparent GWVSS and MAVSS location at 30, 60,

24

90, and/or 120 seconds of more than 30 m are shown in Table 13. These proportions appear to be relatively high. However, several features of this analysis method make it inconclusive. Note that vortex positions are interpolated no more than 15 seconds in Table 13. Thus, if a valid GWVSS measurement exists at 60 seconds but no MAVSS detection occurs between 45-75 seconds, the observation is not considered in this analysis. In addition, to obtain valid vortex velocities, only observations which have MAVSS detections prior to and subsequent to the closest MAVSS detection are used (except in instances where the closest MAVSS detection occurs at the last MAVSS speaker in the line, then the requirement is a detection at the previous speaker. A side effect of this restriction is to bias against inclusion of slow moving vortices and, in addition, to exclude a majority of the observations in the takeoff database from consideration in the analysis. As noted above, the discrepancy between GWVSS and MAVSS is increased with increasing vortex velocity. Thus, this analysis may indicate a higher discrepancy rate than truly exists overall in the takeoff database. Generally, when analysts have compared raw strip chart data for the two systems, they have observed reasonable agreement between the systems. Unfortunately, the manual approach is too cumbersome to provide an overview.

Table 13. Difference (d) between MAVSS and GWVSS Vortex Locations Using MAVSS Extrapolations of Less Than 15 Seconds

Age	B-727	Cases		DC-10	Cases		B-747	Cases	
(s)	d<30m	d>30m		d<30m	d>30m		d<30m	d>30m	
30	214	43	17%	165	61	27%	28	4	13%
60	10	9	47%	28	32	53%	7	11	61%
90	0	1	100%	3	4	57%	0	0	
120	0	0		0	0		0	0	

A more restrictive version of this analysis only permits interpolations of 5 seconds or less (Table 14). Statistics for this more restrictive analysis are only significant for the B-727 and DC-10 at 30 seconds. There is a 20-25% discrepancy rate (proportion of vortices with differences in observed GWVSS and MAVSS location in excess of 30 m) for these aircraft at 30 seconds, representing a slight improvement over the corresponding proportion in the 15 second analysis. The relatively high discrepancy rate, while not conclusive due to biases in choice of data for analysis, is cause for concern in analyses of vortex transport distance probability.

Table 14. Difference (d) between MAVSS and GWVSS Vortex Locations Using MAVSS Extrapolations of Less Than 5 Seconds

Age	B-727	Cases		DC-10	Cases		B-747	Cases	
(s)	d<30m	d>30m		d<30m	d>30m		d<30m	d>30m	
30	89	21	19%	83	18	18%	18	1	11%
60	4	2	33%	3	4	57%	2	1	33%
90	0	0		1	1	50%	0	0	
120	0	0		0	0		0	0	

25

3.5 EXTREME CASES

The probability plots generated during this study will be used to assess crosswind conditions where the probability of a vortex reaching a parallel runway becomes very low. Of necessity, low probabilities involve only a few vortex detections and are therefore very sensitive to the extreme cases of vortex behavior which may be influenced by data anomalies. This section will examine the data validity for such extreme cases. The questions to be answered are:

1. Are the wake vortex measurements valid?

2. Are the wind speed measurements valid?

The extreme cases involve vortices that traveled the farthest and vortices that travel with the least assistance from the ambient crosswind. These cases appear on the tail ends of the probability plots presented above.

Table 15 summarizes the vortices that traveled the farthest. Of the 238 vortices that reached the farthest takeoff MAVSS sensor (at 396 m), only 2 were generated under an adverse crosswind (blowing to the negative side): one from a DC-10 and one from a B-727. Their strengths, as estimated by the MAVSS, were sufficiently low as to render the data suspect. Of the 31 vortices that reached the GWVSS sensor at 472 m, which was not the last sensor, only 10 were independently verified by the MAVSS which was operational for only half the database. The crosswind in all cases was between +2 and +15 knots. Of the 108 vortices (from landing aircraft) that reached the farthest MAVSS sensor (305 m, negative side), none were detected under adverse crosswind conditions (wind blowing to the positive side). It should be noted that, at the distance of 396 m, the GWVSS detected only 0.1% of the total number of vortices, in comparison to 1.4% detected by the MAVSS.

Table 15. Vortices at Farthest Sensors

	TAKEOFF		LANDING
	MAVSS	GWVSS	MAVSS
Farthest sensor (m)	+396	+549	-305
Farthest sensor at which vortex was detected (m)	+396	+472	-305
Number of vortices reaching farthest sensor	238	31	108
Total number of runs in database	8,836	16,878	7,011

Thus, the influence of crosswind on vortex lateral transport is much as expected. Sensor anomalies are the likely source for any vortices with unreasonable transport behavior.

4. EFFECT OF THE GROUND PROXIMITY ON VORTEX MOTION AND LIFETIME

The proximity of the ground has a profound influence on wake vortex behavior, both transport and decay. The takeoff database is appropriate for studying such effects since data were collected for aircraft at varying distances from the ground. A series of SAS analyses used the takeoff MAVSS database to investigate the effect of the ground on vortex motion and lifetime.

The presence of the ground is usually modeled[4] by using an image vortex below each real vortex to satisfy the boundary condition of no vertical wind at the ground. Each image vortex has the same strength as its real counterpart, but with opposite sensor of rotation. The image vortex is centered directly below its real counterpart at a distance below the ground equal to the height of the real vortex.

The image model predicts that the vortex pair will descend to a height of approximately three semispans of the generating aircraft and then begin separating due to ground effect. Thus, for vortices in ground effect, the downwind vortices (termed Vortex 1 in MAVSS analyses) should transport faster than the ambient crosswind, whereas the upwind vortices (termed Vortex 2) should transport more slowly than the ambient crosswind.

The ground will also induce a vertical wind shear resulting from viscous forces acting on the ambient wind. During the Toronto takeoff test[9], the horizontal wind magnitudes were measured at 6- and 30-m heights. For moderate winds between 5 and 10 knots, the windspeeds averaged 1.6 ± 0.9 knots greater at the higher altitude.

The combined effect of the image vortices and the vertical wind shear predicts that the transport speeds of the downwind vortices should generally be independent of vortex height whereas the lateral transport speeds of the upwind vortex should increase with vortex height. The empirical results of Section 4.1 agree with this prediction.

Section 4.2 investigates the effect of the ground on vortex lifetime. In general, the lowest vortices decay most quickly, probably due to friction and/or linking with the ground. Section 4.3 investigates the effect of vortex height on the maximum transport distance of a vortex. This section is a synthesis of Sections 4.1 and 4.2, since maximum transport distance is a function of vortex transport speed and vortex lifetime.

4.1 VORTEX TRANSPORT SPEED

4.1.1 Relative to Ambient Wind

The analysis presented here is akin to the German[10] analysis of Frankfurt Airport data for wake vortices generated on landing. The influence of the ambient crosswind is subtracted from the vortex motion to determine the influence of the ground. The analysis parameter for this section is the difference between the crosswind component of the ambient wind and the vortex transport speed. The signs are selected so that a positive value means that the vortex is moving away from the runway centerline faster than the ambient crosswind. The differences are averaged over all the selected vortices to provide the data included in the figures and tables. The ambient wind measurements were collected at 15-m height on meteorological tower #1, about 500 m from Runway 22L.

27

Figures 9 and 10 show the lateral transport speeds relative to the ambient crosswind for Vortex 1 and Vortex 2; only vortices with at least two MAVSS detections are included to assure reliable transport speeds; transport speeds above 10 m/s were removed as invalid. The data are disaggregated by vortex height and plotted against the crosswind magnitude.

A strong correlation is evident in Figures 9 and 10 between the relative transport speed of the vortices and the magnitude of the ambient crosswind. For low crosswinds, the vortices are transporting on average 4 to 5 knots faster than the ambient crosswind, whereas at higher crosswinds the vortices are transporting at about the same rate as the ambient wind. Most of this correlation is explained by a selection effect caused by a bias in the way the data were selected for inclusion in the averages. Specifically, the requirement for two MAVSS detections requires relative rapid vortex motion and hence, for low crosswinds, will select vortices moving relatively faster than the crosswind. The second MAVSS antenna was located at least 90 m from the runway centerline. Hence, assuming an average vortex age of 60 seconds, the vortices would have to transport at least 1.5 m/s or 3 knots to be included in the average. For low crosswinds there will be many vortices travelling slower than this value that will therefore be excluded from the averages. Certainly, any vortices stalled over the runway, i.e., not detected by any MAVSS antenna, will be excluded from the averages. Note that the bias becomes even worse if longer distance vortex transport is required, e.g., vortex detections at (-244 or +232 m) or +274 m.
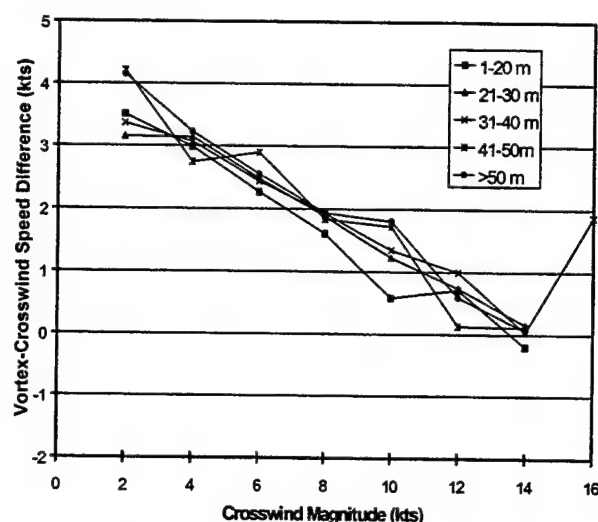
Figure 9. Vortex Transport Speed Relative to Ambient Crosswind, Vortex 1
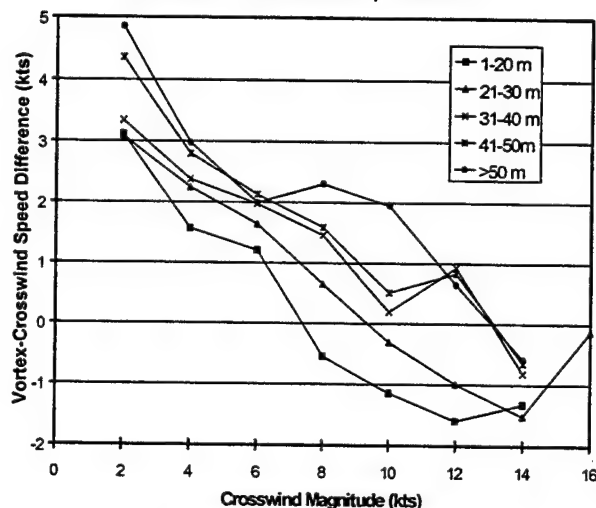
Figure 10. Vortex Transport Speed Relative to Ambient Crosswind, Vortex 2

To remove the selection bias of two MAVSS detections, the analysis was repeated using ambient crosswinds greater than nine knots, where few vortices would be excluded by moving too slowly. The mean and standard deviation (StD) results are listed in Table 16.

Table 16 shows that the relative transport speed for Vortex 1 (downwind) is essentially independent of height (maximum variation of mean is only 0.68 knots). On the average, Vortex 1 transports away from the runway at a speed one knot greater than the ambient wind. The height dependence of Vortex 1 relative transport speeds can be explained by the opposing effects of the image vortex and vertical wind shear. The image vortex (i.e., ground effect) will speed up Vortex 1 most when it is near the

ground and less for higher altitudes. Vertical shear has the opposite effect, speeding up higher vortices more than lower vortices. The combination of opposing effects leads to the observed approximate independence of relative transport speed.

Table 16. Vortex Transport Speed (knots) Relative to Ambient Crosswind with Magnitude above Nine Knots

Vortex Height	Vortex 1			Vortex 2		
	Count	Mean	StD	Count	Mean	StD
0-20 m	164	0.50	2.61	181	-1.42	2.78
20-30 m	334	0.85	2.46	273	-0.80	2.75
30-40 m	221	1.18	2.64	114	0.06	2.99
40-50 m	127	1.13	2.90	103	0.41	3.37
>50 m	163	1.02	3.24	128	1.39	3.12

Table 16 and Figure 10 show a definite height dependence for the relative transport speed of Vortex 2 (upwind). High vortices transport away from the runway about three knots faster than low vortices. This dependence can also be explained by the combined effects of ground effect and wind shear. Low upwind vortices are slowed by both ground effect and vertical wind shear. High upwind vortices are slowed less by ground effect and transported faster by larger crosswinds.

In Table 16, the standard deviation of the relative transport speed is typically three knots. Several stochastic factors could account for this spread:

1. The ambient wind sensor was as much as 800 m from the MAVSS antennas detecting the vortices. The wind difference over that distance can result in a variance in the relative speeds.

2. The ambient wind in the databases is a two-second averaged wind evaluated at approximately 60 seconds from the start of run or at the end of the run for short runs. Thus, the time at which the ambient wind is measured could be as much as a minute different from the time when the vortex transport speed is measured. The averaged winds can vary by several knots over a one-minute time span.

3. The effect of an image vortex will be proportional to its circulation divided by its height. The analysis of this section averages over the aircraft types in the database, varying in size from the relatively small DC-9 to the large B-747. The differences in size, as well as differences in decay rates, result in a spread in transport speeds. Table 17, containing data for only B-727 aircraft, shows somewhat smaller standard deviations; some of the reduction, however, may be related to the removal of the ambient crosswind from the analysis.

4. The 10-m width of the height bins in Table 16 will increase the spread in a bin if there is a height dependency. This effect may account for the slightly larger standard deviations for Vortex 2 than for Vortex 1.

4.1.2 Pair Separation Rate

Another way to measure the effect of the ground on vortex motion is to analyze the separation rate of the vortices from each other as a function of height. Table 17 shows the results of this analysis for the B-727.

The analysis leading to Table 17 consisted of the following steps:

1. Each B-727 takeoff vortex in the time-history* database[11] was examined at adjacent 10-second time points t_i and t_{i+1}, where $i = 1$ to n and $t_1 = 0$ seconds.

2. If both vortex height and lateral position were known at both times for both vortices, then a height/separation-rate observation was added to the dataset:

$$\text{height} = (h_{Pi} + h_{Si})/2 \qquad (6)$$

$$\text{separation rate} = (d_{i+1} - d_i)/10 \qquad (7)$$

where: h_{Pi}/h_{Si} = height of port/starboard vortex at time t_i, and

d_i = lateral distance between the vortices at time t_i.

3. The StD Err column of Table 17 is an estimate of the standard deviation of the measured mean value with N cases relative to the actual mean value obtained in an infinite number of measurements; it is given by:

$$\text{StD Err} = \text{StD}/N^{1/2} \qquad (8)$$

The vortices are seen to begin separating in a statistically significant manner, i.e., Mean > StD Err, at an altitude of 50 to 60 m. Above this height, the vortices effectively do not separate. Below this height, the separation rate increases as the height is reduced and ground effect becomes more pronounced. Since the B-727 semispan is 16.5 m, the observed height threshold of 50-60 m for the onset of vortex separation agrees well with the predicted[4] value of three semispans.

Table 17. Vortex Separation Rate (knots) versus Vortex Height for B-727 Aircraft

Height	N	Mean	StD	StD Err
0-20 m	53	2.02	1.98	0.27
20-30 m	169	1.95	2.45	0.19
30-40 m	96	1.36	2.46	0.25
40-50 m	41	0.76	1.85	0.29
50-60 m	28	0.92	2.26	0.43
60-70 m	12	0.27	0.96	0.28
70-80 m	10	0.37	1.04	0.33
>80 m	7	-0.28	0.22	0.08

The results of Table 17 are consistent with those of Table 16. Both show an averge vortex separation rate of roughly two knots below 30-m height and little separation, if any, above 50 m.

The separation analysis of Table 17 has a major advantage over that in Table 16 in that the ambient wind measurement is not involved. As discussed earlier, the ambient wind measurements can be significantly separated from the vortex measurements in both time and space and hence can introduce additional uncertainty into the analysis.

---

* Interpolates and extrapolates the MAVSS data to give vortex location and circulation every ten seconds, with a total of n data points.

4.2 VORTEX LIFETIME

The MAVSS takeoff database was analyzed to assess the relationship between vortex lifetime and the parameters: (a) vortex height, (b) crosswind magnitude, and (c) vortex position relative to the crosswind direction (downwind or upwind, Vortex 1 or 2). The vortex lifetime was estimated as the time of last vortex detection. If vortex death is defined as the vortex circulation dropping below the MAVSS detection threshold, then the actual lifetime will be longer than the last detection because of the discrete spacing of the MAVSS antennas and the finite length of the antenna array. The potential fractional error is reduced when a vortex is detected by a greater number of antennas. The lifetime is truncated if the vortex drifts off the end of the array. Consequently, the analysis will use only data from the starboard side of the MAVSS array, which has more antennas and a greater maximum distance than the port side (see Table 2). Table 18 presents the results of the analysis. The height for each vortex was taken as an average over all its detections.

No clear dependence on crosswind or vortex number is evident in Table 18. The abnormally high Vortex 2 value

Table 18. Mean Vortex Lifetime (s) as a Function of Height, Crosswind Magnitude (CW), and Vortex Number

Vortex Height	CW<3 (knots)		6<CW<9 (knots)	
	Vortex 1	Vortex 2	Vortex 1	Vortex 2
0-20 m	31	47	24	31
20-30 m	41	48	46	44
30-40 m	50	50	50	40
40-50 m	42	45	43	40
>50 m	42	43	36	38

(47 seconds) for low vortices (0-20 m) and low crosswinds is probably the result of a selection bias in the analysis. In light crosswinds, Vortex 2, which is slowed down by ground effect and has a longer distance to travel than Vortex 1, will take a long time to reach the first MAVSS antenna; no short lifetimes can therefore be observed. In contrast, Vortex 1 is speeded up by ground effect and has a shorter distance to travel; it therefore suffers no selection bias.

On the other hand, Table 18 suggests a height dependence on vortex lifetime. The longest lifetimes are observed for intermediate heights (20-40 m). Low vortices (height < 20 m) have the shortest lifetimes. They are most susceptible to friction and/or linking with the ground. In addition, vortices below 20-m height are typically from smaller aircraft (span < 40 m) since vortices typically descend[4] to a minimum height of roughly one semispan). The vortices above 40-m height also appear to die somewhat more quickly.

4.3 VORTEX TRANSPORT DISTANCE

The same dataset examined in the previous section was analyzed to discover any relationship between vortex transport distance and vortex height, ambient crosswind and vortex number. Table 19 presents the results of this analysis.

Table 19. Mean Distanced (m) Traveled as a Function of Height, Crosswind Magnitude (CW), and Vortex Number

Vortex Height	CW<3 (knots)		6<CW<9 (knots)	
	Vortex 1	Vortex 2	Vortex 1	Vortex 2
0-20 m	90	80	115	100
20-30 m	100	85	145	145
30-40 m	130	95	240	140
40-50 m	115	110	220	140
>50 m	110	105	155	135

31

The trends noted in Table 19 seem reasonable:

1. The vortices travel farther in stronger crosswinds (6-9 knots) than in weak crosswinds (0 to 3 knots).

2. On the Average, Vortex 1 travels farther than Vortex 2. This difference is due to the greater transport speed for Vortex 1 than for Vortex 2.

3. The distance traveled generally increases with vortex height. Two effects are likely responsible, the increase in crosswind with height and the enhanced decay near the ground.

The reduced travel distance (Table 19) and lifetimes (Table 18) for the highest vortices is not readily explained by wake vortex physics. One possible explanation is that the MAVSS vortex detection sensitivity decreases with height, perhaps because of the greater beam width.

5. CHARACTERISTICS OF LONG-DISTANCE VORTICES

Wake vortices that have traveled the greatest lateral distances are most likely to present operational problems for parallel runway operations. This chapter examines the characteristics of the wake vortices that traveled to the most distant MAVSS antenna (+396 m) of the takeoff test. The characteristics of these vortices are compared to those of all the vortices that traveled in the same direction.

In principle, vortex strength can be used to determine whether a vortex poses a hazard to a following aircraft. In practice, it has been difficult to obtain agreement on an acceptable strength threshold,

Table 20. Circulation Hazard Thresholds

Span of Following Aircraft (m)	10	20	40
Circulation Averaging Radius (m)	5	10	20
Circulation Hazard Threshold (m^2/s)	30	60	120

below which a vortex can be considered benign. This chapter will utilize the hazard model used in previous studies[11] (Table 9 of Ref. 11 with f=0.6). Table 20 lists the hazard parameters, which depend upon the wingspan of the following aircraft. Since no agreement exists on acceptable circulation levels, in this chapter, vortices with circulation above the values in Table 20 will be termed "strong."

The SAS set of strong vortices at 396-m lateral position (termed "strong, long" in the following plots) consists of 32 downwind (Vortex 1) and 13 upwind (Vortex 2) vortices. [See Table 24 for the somewhat different Paradox results.] These "strong" vortices will be compared with the set (3229) of all vortices detected on the starboard side of the runway (termed "all" in the following plots). The parameters affecting vortex transport will be identified by comparing their values for the two datasets.

5.1 TIME-OF-YEAR EFFECT ON VORTEX TRANSPORT

Figure 11 compares the day-of-year distribution for strong 396-m vortices with all starboard-side vortices. The distribution is similar for both datasets, with most of the vortices occurring in the fall, during the peak of the data collection. The day numbers in Figure 11 start at the beginning of the year and are grouped in bins of 30 days, corresponding approximately to one month.

5.2 HOUR-OF-DAY EFFECT ON VORTEX TRANSPORT

Figure 12 shows the hour-of-day distributions for the two datasets. The bins are labeled with the midpoint of the time bin, i.e., hour 12 represents local times between 11:30 and 12:30. Note that data collection occurred only during normal working hours. Although the distributions are similar, there is a general indication of relatively fewer strong, long-distance vortices in the middle of the day (hours 12-14). Several possible explanations for this effect are:

1. The starboard crosswinds at O'Hare may be generally weaker in the afternoon. Figure 13 analyzes this possibility; it compares the hour-of-day distribution for vortices with crosswind greater than 8 knots with that for all starboard-side vortices. The strong crosswinds probability shows some reduction relative to all cases for hours 12-13, but not as much as the distribution of long-distance strong vortices. Thus, lower crosswinds may account for part but not all of the reduction noted for hours 12-14 in Figure 12.

33

2. Fewer Heavy aircraft may be scheduled in the afternoon. Figure 14 analyzes this possibility; it compares the hour-of-day distribution for Heavy departures with that all starboard-side vortices. The Heavy-departure probability shows some reduction relative to all cases for hours 12-14, but not as much as the distribution of long-distance strong vortices. Thus, fewer Heavies may account for part but not all of the reduction noted for hours 12-14 in Figure 12.

3. The atmosphere is more turbulent in the afternoon and may lead to enhanced vortex decay. Solar heating generally leads to higher turbulence levels in the afternoon than in the morning.

These three explanations together can account for the observed mid-day reduction in long-distance, strong vortices.
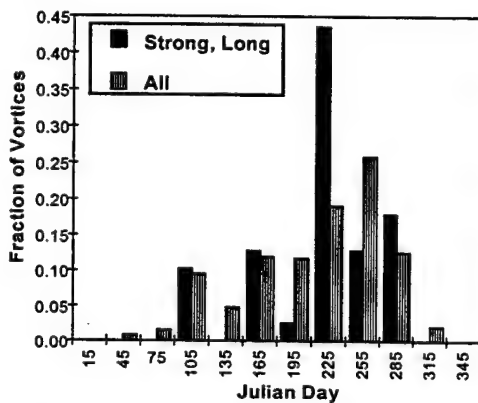
Figure 11. Day-of-Year Distribution
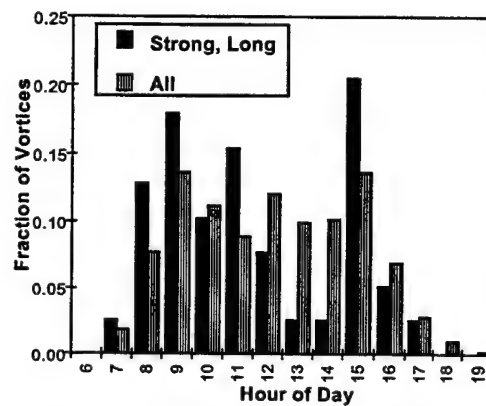
Figure 12. Hour-of-Day Distribution
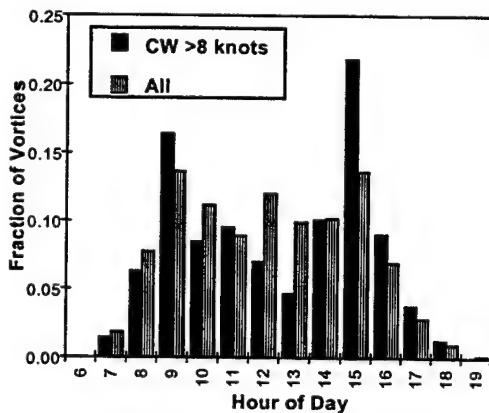
Figure 13. Comparison of Hour-of-Day Distributions for High Crosswinds and All Starboard-Side Cases
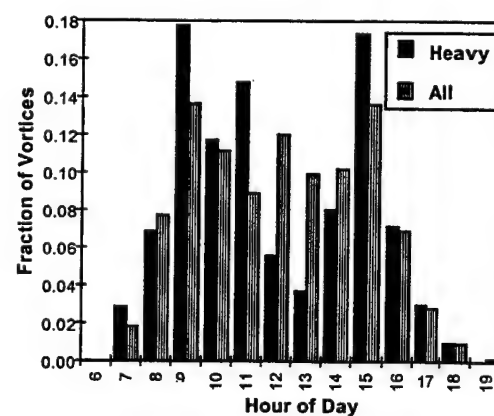
Figure 14. Comparison of Hour-of-Day Distribution for Heavy Departures and All Starboard-Side Cases

34

5.3 SUNSHINE EFFECT ON VORTEX TRANSPORT

Figure 15 compares the distribution of pyranometer readings for long-distance strong vortices with that for all starboard-side vortices. The pyranometer measures the solar radiation in calories per unit area per unit time (solar insolation). The pyranometer values in the database have been observed to correlate strongly with the general weather observations entered by data collection personnel into on-site log books and subsequently entered into the database. Pyranometer readings were generally low during periods of clouds or precipitation and high during sunny weather. The pyranometer values also have a strong diurnal signature with low readings in early morning and late afternoon and maximum readings during midday.

The pyranometer distributions in Figure 15 appear to be roughly uniform and generally similar to each other. The incident sunlight appears to have no appreciable direct influence on the lateral transport of strong vortices.

5.4 CROSSWIND EFFECT ON VORTEX TRANSPORT

Figure 16 compares the crosswind distribution for long-distance strong vortices with all starboard-side vortices. Since positive crosswinds blow toward the starboard side, it is not surprising that most of the crosswinds are positive. The median crosswind for long-distance hazard vortices is eight knots while that for all starboard-side vortices is only four knots. Vortices generally transport farther in a stronger crosswind.
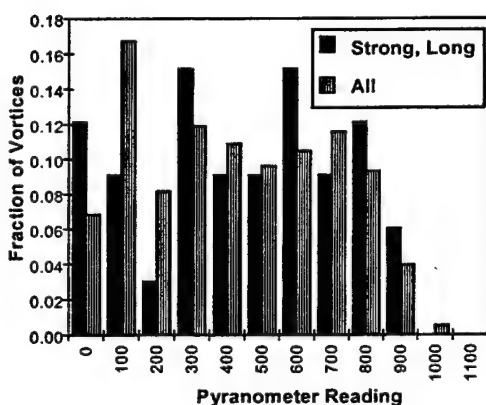
Figure 15. Pyranometer Distribution
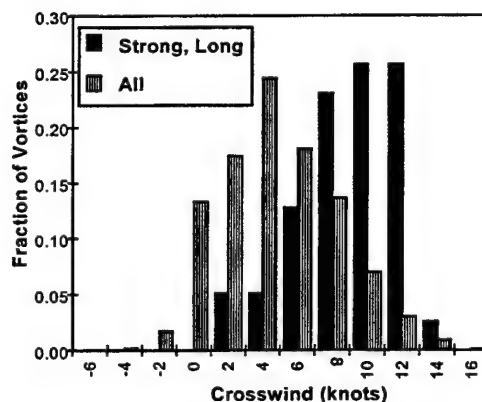
Figure 16. Crosswind Distribution

Figure 16 shows that, in a two-knot crosswind, two vortices (both downwind, Vortex 1; SAS Runs 2 and 4 in later Table 24) were able to transport to the end of the MAVSS array while remaining strong. Table 21 lists the variation in the crosswind relative to the start of run (i.e., time aircraft crossed MAVSS line) for those cases. Table 22 lists the complete MAVSS data for these two runs.

The Table 21 crosswinds decrease from four to two knots from 30 seconds before the start of run to 60 seconds after the start of run, the latter being the value used in the database to characterize the ambient wind for the run. Thus, the ambient wind measurement, which was relatively close to the starboard

35

end of the MAVSS array, suggested that the crosswind was dropping during the run. The highest ambient crosswind of four knots is less than half of most of the transport speeds noted in Table 22.

The analysis of Table 16 showed that, for relatively high crosswinds, the Vortex-1 transport speed for vortex heights of 20-30 m was typically one knot faster than the ambient crosswind with a standard deviation of 2.5 knots, which is much less than observed for these two cases. However, both are Heavies and descend to relatively low altitudes before rising and hence would likely obtain a greater ground-induced speedup; the observed transport speeds have no clear dependence on vortex height, however. The two cases have quite different characteristics:

Table 21. Crosswinds (knots) for Two Extreme Cases

Tape/Case	39/50	43/79
Aircraft Type	L1011	DC-10
CW at -30 s	4	4
CW at 0 s	3	4
CW at 30 s	2	4
CW at 60 s	2	2

Table 22. MAVSS Data for Two Extreme Cases

Location (m)	61	91	232	274	335	396
L1011 Vortex						
Time (s)	9	15	41	50	62	74
Height (m)	32	29	20	23	26	17
Speed (knots)	10	10	10	10	10	10
Circulation (10-m) (m²/s)	152	121	119	99	92	67
DC-10 Vortex						
Time (s)	17	32	71	79	88	95
Height (m)	37	35	20	17	26	29
Speed (knots)	4	6	9	11	15	18
Circulation (10-m) (m²/s)	137	101	83	69	75	79

1. The L1011 case looks fairly normal. It has a constant transport speed of 10 knots and shows a regular height variation except for the sudden height and circulation drop at the last antenna (perhaps related to the Crow instability).

2. The DC-10 case looks more unusual. The transport speed increases dramatically from 4 to 18 knots through the run. The height and circulation variations are more normal, however. The apparent increase in crosswind just as the vortex is getting closer to the wind tower (the wind tower was fairly close to the last MAVSS antenna) seems odd since the tower shows a decreasing crosswind at the same time.

Obtaining close correlation between vortex transport speeds and ambient wind measurements appears to be difficult.

5.5 HEADWIND/TAILWIND EFFECT ON VORTEX TRANSPORT

Figure 17 compares the headwind distribution for long-distance strong vortices with all starboard-side vortices. The headwinds are predominantly positive since aircraft usually take off into a headwind.

Both distributions in Figure 17 have about the same median headwind (about four knots). Strong, long-distance vortices have a narrower headwind distribution than all starboard-side vortices. The loss of strong, long-distance vortices for tail winds is likely a geometrical effect; tailwinds lead to the detection of vortices generated at lower heights, which tend to decay faster (see Section 5.7). The loss of strong, long-distance vortices for high

Figure 17. Headwind Distribution

36

headwinds may represent the influence of the accompanying high turbulence in promoting faster vortex decay.

5.6 AIRCRAFT TYPE EFFECT ON VORTEX TRANSPORT

Figure 18 compares the aircraft type distribution for long-distance strong vortices with all starboard-side vortices. The aircraft are arranged in order of increasing size.

Figure 18 shows clearly that aircraft size has a strong influence on whether wake vortices will reach the last MAVSS antenna and remain strong. This result is expected and is, in fact, the basis for the use of aircraft size classes to define separation standards.

Figure 18. Aircraft Type Distribution

5.7 AIRCRAFT HEIGHT EFFECT ON VORTEX TRANSPORT

Figure 19 compares the aircraft height distribution for long-distance strong vortices with all starboard-side vortices. The aircraft height was determined photographically as the aircraft crossed the MAVSS antenna line.

Figure 19 shows clearly that aircraft height has a strong influence on whether wake vortices will reach the last MAVSS antenna and remain strong. Long-distance, strong vortices were observed:

1. Never for heights below 100 feet (30 m)

2. With reduced probability for heights below 150 feet (46 m), but

3. With more than twice the probability for heights above 225 feet (69 m).

The predominance of higher aircraft heights for strong, long-distance vortices is generally consistent with Table

Figure 19. Aircraft Height Distribution

19, which shows that, below 50-m vortex height, the mean vortex transport distance increases with height. The consistency in Figure 19 of higher transport probabilities for higher altitudes again suggests that the reduced mean transport distance in Table 19 for vortices above 50-m height is an instrumental, not a physical effect.

One way to confirm the influence of aircraft height is to analyze the distribution of aircraft altitudes as they passed Line A during takeoff. Line A was located[2] 580 m before the MAVSS line. The on-site operator noted in the daily log the attitude of each aircraft at Line A: on ground (OG), nose up (NU), airborne (AB) or gear up (GU).

Figure 20 compares the aircraft Line-A attitude distribution for long-distance strong vortices with all starboard-side vortices.

37

In Figure 20, the distribution for long-distance, strong vortices is displaced to higher altitudes than that for all starboard-side vortices. Almost none of the aircraft generating long-distance, strong vortices were on the ground. This result is consistent with the height analysis in Figure 19 and serves to establish the validity of both the photographic data reduction and the logging of aircraft attitudes. Both data sources indicate that the aircraft must be above some minimum altitude at vortex generation to produce strong vortices with long lateral transport.

5.8 DIFFERENCES BETWEEN UPWIND AND DOWNWIND VORTICES

Table 23 lists the number vortices detected for each run for two groups: long-distance, strong vortices and all starboard-side vortices. The long-distance, strong vortices usually (67 %) have only Vortex 1 detected. On the other hand, the runs with starboard-side vortices usually (56 %) have both vortices detected.

The major reason for the deficit of strong upwind vortices (Vortex 2) at the last MAVSS antenna is that they take longer than downwind vortices (Vortex 1) to get there (longer distance by almost one wingspan and slower transport speed) and hence have more time to decay. Figure 21 compares the ages of the strong downwind (Vortex 1) and upwind (Vortex 2) vortices at the last MAVSS antenna. The upwind vortices are typically ten seconds older.

Figure 22 shows the circulation decay for DC-10 wake vortices; the DC-10 was the Heavy aircraft with the most data. The average of the circulation for vortex radii between 10 and 20 meters is used to estimate the total circulation. The measurements for each vortex are plotted as boxes and connected with lines. The circulation values for Vortex 1 and Vortex 2 are plotted as negative and positive values, respectively. In contrast to landing[11] where the lifetime of Vortex 2 was typically longer than that of Vortex 1, the takeoff data show more or less similar decay for both vortices. Consequently, the difference in travel time for Vortex 1 and 2 are the primary reason for the predominance of Vortex 1 in the strong vortices which have reached the last MAVSS antenna.
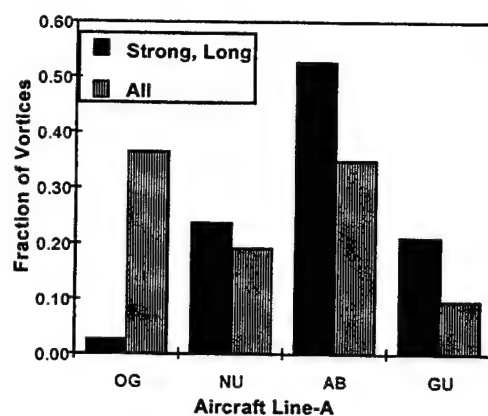
Figure 20. Aircraft Line-A Attitude Distribution

Table 23. Number Vortices Detected

Vortex	Long, Strong Runs	All Stbd. Side Runs
Only 1	26 (67%)	1488 (34%)
Only 2	7 (18%)	38 (1%)
Both	6 (15%)	1923 (56%)
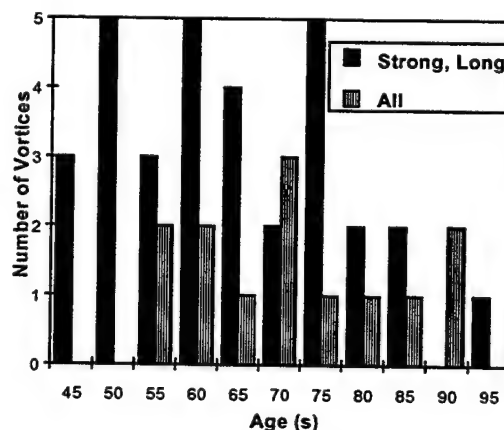
Figure 21 Age Distribution

38
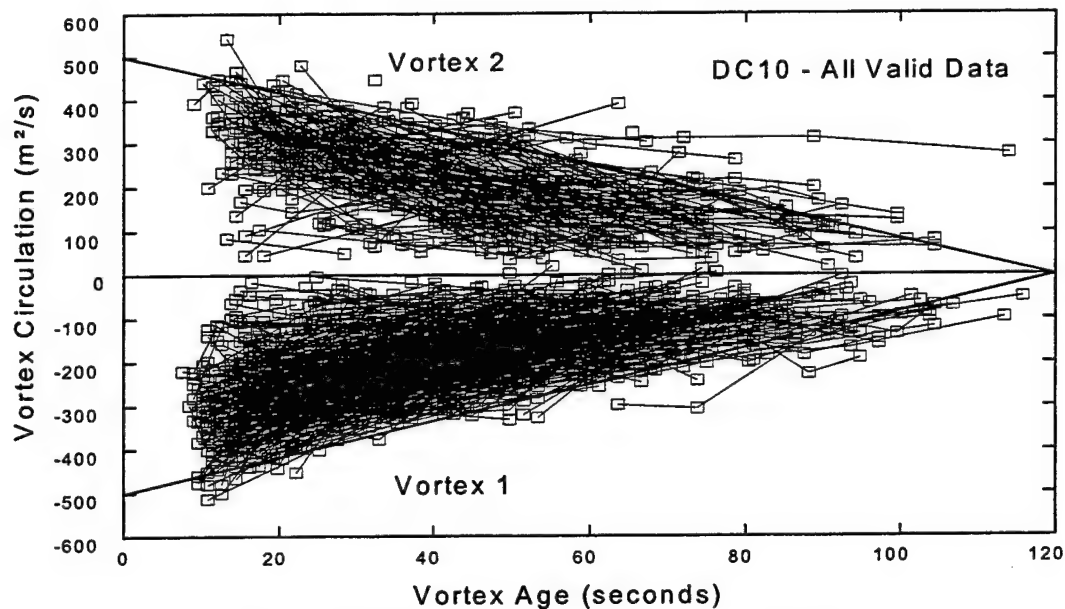
Figure 22. Takeoff Circulation Decay for DC-10

5.9 VORTEX HEIGHTS

Figure 23 compares the average height distributions of the strong downwind (Vortex 1) and upwind (Vortex 2) vortices reaching the last MAVSS antenna to the corresponding height +distributions for all starboard-side vortices. The height average is over all the detections of a particular vortex.

The all starboard-side Vortex 1 and Vortex 2 height distributions in Figure 23 are similar. The long-distance, strong vortices have slightly higher typical heights for Vortex 1 and significantly higher heights for Vortex 2.
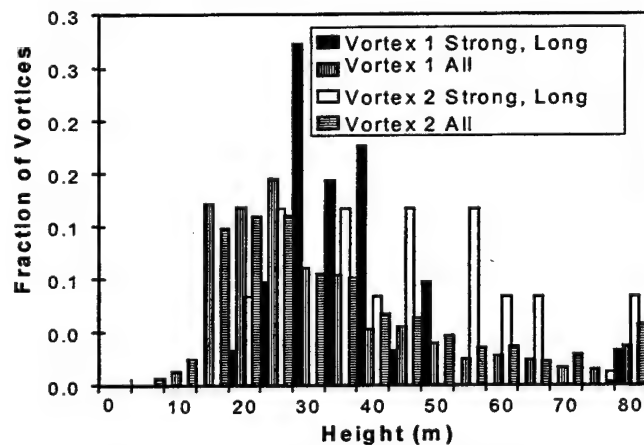
Figure 23. Average Height Distribution

5.10 VORTEX HEIGHT PROFILES

The average height data in the previous section masks the actual motion of individual vortices. This section examines whether, in general, vortices that remain strong at the last MAVSS antenna are rising, falling, or remaining at a fixed height. Table 24 lists the height profiles for all 65 vortices that were still potentially strong at the last MAVSS antenna. The heights (m) are labeled by the lateral position in meters, e.g., H396 for the last MAVSS antenna. Naturally, all the vortices had height values for H396. Missing vortex detections show up as blank height values. Zero height values indicate manual editing of a detection with correct time but incorrect height. The aircraft height is listed in the column labeled HAC.

39

The vortices in Table 24 came from the Paradox databases listed in Appendix C. The vortices were selected using the three strength levels listed in Table 20 for average circulations with radii of 5, 10 and 20 m. The Columns S5, S10 and S20 specify whether each level was reached (Y or N) at the last detection. The total number of vortices reaching at least one strength threshold was significantly greater than in the original SAS analysis (45 vortices). Only 37 of the original 39 SAS runs showed up in the current Paradox analysis; the run numbers of the SAS analysis are listed in the last column of Table 24. No obvious explanation can be discerned for the differences between the SAS and the Paradox selections. Where a SAS run number is listed, the classification of the height profile is taken from the original SAS analysis. [The observed discrepancy of the SAS and Paradox selection of strong, long-distance vortices casts some doubts on the analysis of this chapter. Most of the plots were derived from the original SAS analysis. A few SAS plots were lost or unusable and had to be reconstructed using the Paradox databases.]

Each vortex height profile was classified into one of seven classifications:

Low: The vortex height remains generally below 30 m during the entire transport out to 396 m. These vortices will be experiencing a strong ground effect during their entire lifetime.

Medium: The vortex height remains generally in the 30 to 35 m range during the entire transport out to 396 m. The presence of the ground will have a moderate effect on these vortices during their entire lifetime.

High: The vortex height remains above about 35 m during the entire lifetime of the vortex. The presence of the ground will have a minimal effect on these vortices.

Rising: The general trend of vortex heights is decreasing with the average of the last two heights generally at least 10 m higher than the average of the first two heights. The vortex is initially in ground effect and rises out of ground effect.

Falling: The general trend of vortex heights is decreasing with the average of the last two heights at least 10 m below the average of the first two heights. The vortex is initially out of ground effect and descends into ground effect.

Curved: The vortex starts out of ground effect, descends into ground effect, and then rises out of ground effect. The average of the first and last heights are at least 10 m above the lowest height.

Miscellaneous: The height profile does not match any of the above six descriptions.

Table 24. Height Profiles for Strong Vortices Reaching 396-m Antenna

RECID	A/C	VN	S5	S10	S20	H396	H335	H274	H232	H91	H61	HAC	SAS	Class
80-04-17:09:10:23	747	1	Y	Y	Y	41	37	35	32	23		-1	1	Ris
80-04-17:09:17:50	L1011	1	Y	Y	N	17	26	23	20	29	32	-1	2	Low
80-04-21:08:39:55	747	1	N	Y	N	58	43	41	37	23		30	3	Ris
80-04-21:10:33:48	DC-10	1	Y	Y	Y	29	26	17	20	35	37	76	4	Curv
80-06-23:10:34:50	DC-10	1	Y	Y	Y	17	26	29	37	81	72	61	5	Fall
80-06-23:12:01:01	L1011	1	Y	N	N	29	32	35	26	29	26	46	6	Low
80-06-23:12:04:36	DC-10	1	N	Y	N	35	0	29	32	29	32	46	7	Med
80-06-24:09:46:08	DC-10	1	Y	N	Y	35	32	29	37	64		61	8	Fall
80-06-24:14:42:45	DC-8 H	1	Y	N	N	29	26	23	26	52		61	9	Curv
80-06-31:09:07:28	DC-10	1	Y	Y	Y	35	60	29	32	23		30		
80-07-17:10:34:49	DC-10	1	Y	N	N	35	26	23	20	29		46	10	Curv
80-07-29:10:44:17	DC-10	1	Y	Y	N	35		23				-1	11	Ris
80-07-29:11:08:02	727	1	N	Y	N	35	37	29	37	23		-1		
80-07-29:11:08:02	727	2	Y	Y	N	29	32	23	26	23		-1	12	Ris
80-07-29:13:24:17	DC-10	1	Y	N	N	58	32	29	32	23		-1		
80-07-29:14:11:46	727	1	Y	N	N	17	20	46	37	69	60	-1	13	Fall
80-07-29:14:16:53	727	2	Y	N	N	17			20	23	37	-1		
80-07-29:15:00:35	DC-10	1	Y	Y	Y	46	55	52	55	69		76		
80-07-29:15:00:35	DC-10	2	Y	Y	Y	29	32	29	32	58	60	76		
80-07-29:15:16:33	DC-10	1	N	Y	Y	23	26	23	26	23		38		
80-07-29:15:16:33	DC-10	2	Y	Y	Y	17	20	17	14	23	20	38		
80-07-29:15:18:26	727	2	Y	Y	N	46		58	72	93		107	14	High
80-07-29:15:26:17	DC-10	1	Y	Y	N	29	26	29	37	58		61	15	Fall
80-07-29:15:27:29	707 H	1	N	Y	N	17	26	35	43	81		91	16	Fall
80-07-29:15:27:29	707 H	2	Y	Y	N	23	26	29	37	69	72	91	16	Fall
80-07-29:15:51:25	747	1	Y	N	N	35	26	23	20	41		53	17	Curv
80-08-04:07:55:42	DC-10	1	Y	N	N	41	37	35	32	41	43	61	18	Curv
80-08-04:07:55:42	DC-10	2	Y	Y	Y	17	26	29	26	23	32	61	18	Low
80-08-04:09:16:48	DC-10	1	N	Y	Y	35	43	52	37	58	72	76	19	High
80-08-04:09:36:07	727	1	N	Y	N	35	37	29	37	29		61		
80-08-04:09:48:28	DC-10	1	Y	Y	Y	93						122	20	High
80-08-04:09:48:28	DC-10	2	N	N	Y	93						122	20	High
80-08-04:10:36:12	DC-10	1	Y	Y	N	35	37	29	26	23		30	21	Ris
80-08-04:12:25:34	DC-10	1	Y	N	N	46	37	35	32	0		38	22	Misc
80-08-04:15:03:59	707 H	1	Y	Y	N	52	55	46	49	46	0	61	23	High
80-08-04:15:58:35	DC-8 H	1	Y	Y	Y	17	26	23	20	23	26	30	24	Low
80-08-04:15:58:35	DC-8 H	2	Y	Y	N	23		23	20	17	20	30	24	Low
80-08-04:16:57:06	747	1	Y	Y	N	41	43	35	32	23	20	30		
80-08-04:17:11:28	DC-10	1	N	Y	N	29	26	29	32	58	55	69	26	High
80-08-07:07:51:25	DC-10	2	Y	N	N	35	43	46	43	58	60	69	27	High
80-08-07:07:58:11	DC-10	2	Y	Y	Y	58	60	58	60	58	66	69	28	Curv
80-08-28:14:48:49	DC-8 H	1	Y	Y	Y	29	26	17	32	35	37	53	30	Misc
80-09-12:14:35:49	727	2	Y	N	N	29		52		35		46		
80-09-22:10:07:50	DC-9	2	Y	N	N	35						46	31	High
80-09-24:09:34:30	707	1	Y	Y	Y	41	43	52	55			76	31	Fall
80-09-24:09:34:30	707	2	Y	Y	N	29	37	52	60	93		76	32	Ris
80-09-24:10:34:27	DC-10	1	Y	N	N	41	0	35	37	17	20	38	33	Curv
80-10-14:07:46:14	DC-10	1	Y	N	N	35	32	29	32	52		-1	34	Ris
80-10-14:08:21:36	747	1	Y	Y	N	52	43	41	37	23		-1	35	Ris
80-10-14:09:18:36	DC-10	1	Y	Y	N	35	37	23	26	17		-1	36	Low
80-10-14:09:25:06	707	1	Y	N	N	29	26	29	32	29		-1	37	Fall
80-10-14:09:52:43	727	2	Y	Y	Y	35	26	29	32	46	49	-1		
80-10-16:15:12:50	DC-10	1	Y	Y	N	41	37	41	20	29		46		
80-10-24:07:24:56	DC-10	1	Y	Y	N	23	37	35	37	64		76	38	Fall
80-10-24:07:24:56	DC-10	2	N	Y	N	41	14	29	37	58		76	38	Curv
80-10-24:07:44:04	DC-10	1	Y	Y	Y	58	55	69	72	87		107		
80-10-24:07:44:04	DC-10	2	Y	Y	Y	93	84	64	72	87		107		

Table 24. Height Profiles for Strong Vortices Reaching 396-m Antenna (cont.)

80-10-24:07:47:40	727	1	N	Y	N	46	49	64	14		43	91		
80-10-24:07:59:12	DC-8 H	1	Y	Y	Y	75	78	41	66			91		
80-10-24:08:14:23	DC-9	1	Y	Y	N	87	66	87	43			91		
80-10-24:08:14:23	DC-9	2	Y	Y	Y	75	72	81	66	93	78	91		
80-10-24:08:20:34	DC-8 H	1	Y	Y	Y	93	95	0	66			91		
80-10-24:09:18:00	DC-10	1	Y	Y	N	35	26	35	32	35		46	39	Med
80-10-24:09:19:36	727	2	N	Y	N	52			49	69		91		
80-10-24:10:36:52	DC-10	1	Y	N	N	35	26	41	26	29	37	61		

Note that SAS Runs 25 (Falling Vortex 2) and 29 (Falling Vortex 2) were not found.

Table 25 lists the number of vortices in each height profile class (from the original SAS analysis). From Table 25 it is clear that vortices can follow a great variety of different trajectories as they transport out to large distances. The majority, however, consist of vortices that undergo a height change (falling, rising or curved) during their lateral transport. Sixty percent of the long-distance, strong vortices underwent a height change. The height changes resulted either from high takeoffs with the vortices out of ground effect initially and eventually descending into ground effect or from downwind vortices initially in ground effect and then rising out of ground effect because of wind shear. In both cases, proximity to the ground *for a limited time* appears to increase the likelihood of long lateral transport.

Table 25. Number of Vortices in Each Height Profile Class

Class	Vortex 1	Vortex 2
Low	4	2
Medium	2	0
High	4	4
Falling	5	6
Rising	8	0
Curved	7	1
Miscellaneous	1	1

5.11 SUMMARY

The results presented in the previous subsections indicate the stochastic nature of vortex transport. Strong vortices can transport out to 396 m or more under a variety of different weather conditions and aircraft types.

However, some patterns for several typical cases where there is a greater potential for long distance transport of a strong vortex. One typical case is a Heavy aircraft taking off in a moderately strong crosswind where the downwind vortex rises due to wind shear and transports a long distance. Another typical case is a Heavy aircraft with a high takeoff in a moderately strong crosswind. The two vortices descend into ground effect as they are laterally transported by the ambient wind. They eventually are separated by ground effect and one or both transport a long distance.

6. SUMMARY OF RESULTS

6.1 TRANSPORT PROBABILITY.

As shown in Figures 3 through 5, the probability of a vortex reaching a given distance generally increases as the crosswind increases in that direction. The probability drops off very sharply once the crosswind blows in an adverse direction (i.e., a negative crosswind for a vortex reaching a sensor on the positive side).

For a given crosswind range, the probability of a vortex reaching a certain distance from the runway centerline decreases as that distance increases. In many cases, the log of the probability is proportional to the distance squared.

6.2 COMPARISON OF MAVSS AND GWVSS RESULTS

In a previous report[2] the MAVSS and GWVSS estimates of vortex transport probability were compared without crosswind restrictions by estimating how many vortices traveled in each direction from the runway centerline. The analysis in this report used crosswind restrictions and did not set any limits on the direction of vortex motion.

A comparison of Figure 8 with Figure 6 shows that the GWVSS plots have substantially lower probabilities for vortex transport than do the MAVSS plots. However, the landing (Figure 7) and takeoff (Figure 6) MAVSS probabilities are more or less comparable. Table 6 compared the results for all three types of data and the three aircraft types for a particular choice of distance and favorable crosswind. The decay rates for the DC-9 and B-727 were comparable, but significantly greater than that for the DC-10.

Although the MAVSS probability (Figures 3 and 4) does not decrease significantly for large favorable crosswinds, the GWVSS probability (Figure 5) does decrease somewhat, presumably because of lower GWVSS detection sensitivity in high crosswinds.

The analysis of Tables 8 through 10 suggests that the MAVSS and GWVSS are approximately equivalent for tracking *low altitude* vortices under *low wind* conditions. For example, for 67 percent of the B-727 vortices between 10- and 19-m altitude, the GWVSS death position is beyond the last MAVSS detection Table 26 extends this analysis by using total wind magnitude (rather than crosswind magnitude), which should be a better surrogate for turbulence level. The analysis excluded MAVSS cases with last detection at the end of the line and, of course, required a valid GWVSS measurement of death position. As the wind magnitude is limited to lower and lower values, the all-cases probability of 69 percent climbs to 92

Table 26. B-727: Probability of GWVSS Death Position at Distance ≥ Last MAVSS Detection

Wind Magnitude	Cases	Percent
unlimited	2198	69
<9 kts	1496	73
<7 kts	1082	76
<5 kts	684	80
<4 kts	490	82
<3 kts	335	84
<2 kts	207	89
<1 kts	62	92

percent for wind magnitudes below one knot. The analysis was insensitive to limits on aircraft height; if the aircraft is low enough for the GWVSS to detect a vortex at all, the relative values of MAVSS and GWVSS vortex lifetime are unaffected by aircraft height.

43

6.3 EXTREME CASES

The influence of crosswind on vortex lateral transport is much as expected. Sensor anomalies are the likely source for any vortices with unreasonable transport behavior.

6.4 EFFECT OF GROUND PROXIMITY

Ground proximity results in greater vortex separation rates (Table 17) and faster vortex decay (Table 18).

6.5 CHARACTERISTICS OF LONG DISTANCE VORTICES

Long-distance, strong vortices are mostly Heavies (see Table 24, Figure 18) and are typically generated at higher altitudes (Figure 19) and higher crosswinds (Figure 16) than vortices with shorter transport distances. This effect is consistent with vortex decay being accelerated by interaction with the ground.

7. CURRENT CONSIDERATIONS AND RECOMMENDATIONS

7.1 DATA COLLECTION

Recent airport data collection efforts have made a number of improvements, which were facilitated by the tremendous improvements in computer and communication technology in the last 20 years. At present, only the GWVSS has been updated and deployed because of (a) its all-weather capability, (b) its relatively low data rates, and (c) its relatively low costs. In the future, the MAVSS may also be updated and deployed, if funding can be obtained.

7.1.1 GWVSS Improvements

Recent GWVSS installations have built on the German work of the 1980s; the Frankfurt GWVSS installation consisted of three-axis anemometers at 10-m height [the currently active GWVSS at Frankfurt has sonic anemometers at 15-m height]. The taller poles detect a significant vertical vortex wind component and thereby improve the vortex location capability of the system.

7.1.2 Automatic Data Collection

One of the major expenses of the O'Hare data collection efforts was the need to man the site. This requirement translated into data collection during normal business hours. Vortex behavior in the early morning, evening, or night cannot be studied using the O'Hare databases. The primary duties of the site operator were to turn on and checkout the equipment, replace data tapes when full, and make observations on aircraft type. The specific times of aircraft passage were determined automatically by aircraft noise sensors.

Automating the GWVSS data collection required relatively few changes. The data rate was reduced by generating two-second averages before storing the measurements; the resulting data rate is only five Mbytes per day. Current disk capacities can easily store a year's data. Data files are downloaded from the test site on a daily basis and checked for data quality. The only real problem is obtaining the aircraft types. Several approaches have been used:

1. Airport Arrival Records - Matching airport records and acoustic arrivals can be complicated by the one-minute resolution of the airport records and occasional errors in the airport times.

2. FAA Data - Access permission can be difficult and the data processing is complicated.

3. Mode-S Squitter - Passenger aircraft broadcast a Mode-S code that uniquely identifies the aircraft. US aircraft types can then be determined by looking up the code in a database. Foreign aircraft databases are not readily available and cargo aircraft do not have Mode-S.

7.1.3 Real-Time Data Processing

The data are processed in real time using a multitasking operating system and a computer network. The GWVSS anemometer signals are processed to give mean and standard deviations on a minute by minute basis, as well as turbulence estimates with a ten-minute average. Aircraft arrivals are triggered by an aircraft noise detector and used to generate a run file containing all the data for a run. The current two-second data file can be accessed to generate real-time displays of wind fields and estimated wake vortex locations.

45

7.2 DATA ANALYSIS

7.2.1 Ambient Wind from Ground-Wind Anemometers

Using the ground-wind anemometers themselves to estimate the ambient wind should give a more accurate estimate of ambient wind conditions than could be obtained from a distant anemometer. However, the influence of wake vortices on the ambient wind estimate must be eliminated; several algorithms have been developed for that purpose. The use of two-second wind averages for the O'Hare databases also contributes to the variance in the comparisons of crosswind and vortex lateral transport speed. Current studies use a one-minute average.

The possibility of reprocessing the O'Hare takeoff tapes was investigated. The tapes are still available, but the minicomputer format information has been lost. Reconstructing the data would therefore require considerable sleuthing. The ground-wind anemometers of the O'Hare takeoff test provide a potentially useful dataset on the crosswind variance over a large portion of an airport.

7.2.2 GWVSS Processing Algorithms

Current algorithms estimate the ambient crosswind as the median of the array of crosswind measurements. The vortex-induced crosswind (VICW) is taken as the difference between the maximum or minimum crosswind and the median and has been found to be a robust parameter to estimate the quality of the vortex detection. Thresholds on VICW are used to start and stop tracking the vortices. The thresholds are adjusted according to the ambient crosswind turbulence level (ten-minute mean) to avoid false identifications of turbulence as vortices.

The GWVSS processing used for the O'Hare databases made no attempt to extract vortex height or circulation from the measurements. Recent processing algorithms use a least-square fit to estimate height, circulation and to refine the lateral position from the first estimate as the location of the anemometer with the highest or lowest crosswind reading. The height and circulation estimates are much less accurate than the lateral position estimates.

7.3 CURRENT AND FUTURE GWVSS INSTALLATIONS

The current GWVSS installations at JFK and DFW airports extend out to 107 and 152 m, respectively. The DFW data may be marginally useful for parallel runway considerations; a first analysis has looked at the time for vortices to reach 150-m lateral position.

Current 1999 plans call for extending the JFK GWVSS to at least 300-m lateral position and to install a new GWVSS around the landing area of closely-spaced (229 m) parallel runways (28L and 28R) at SFO airport.

7.4 APPLICATION OF RESULTS

The current philosophy for improving procedures for closely-spaced (i.e., closer than 2500 feet) is to use vortex transport characteristics to avoid any wake vortex encounters. The results of this report are encouraging for this purpose.

As might be expected, the probability of a vortex transporting a certain distance becomes high for large favorable crosswinds. Conversely, the transport probability drops sharply for low favorable crosswinds and becomes vanishingly small for crosswinds blowing in the opposite direction. Thus, preliminary indications look promising for a possible parallel-runway procedure where simultaneous parallel runway operations would be conducted with the larger aircraft using the downwind runway.

At a distance of 396 m (the limit of the MAVSS sensors), there were no vortices of any significant strength when the crosswind was blowing in the unfavorable direction. Thus, an aircraft using a runway at least 400 m upwind from a second runway, would appear to be unaffected by any vortex generated at that second runway - even by a Heavy plane such as a DC-10. The DC-10 data in Figures 3 and 4 suggest that this operating rule could be valid for runway spacings as low as 200 m.

7.5 FUTURE ANALYSIS

The analysis[11] of MAVSS landing data led to a vortex duration probability that can be used to define safe longitudinal spacings[12] for a single runway for a particular pair of aircraft. Similar logic could be used to estimate what parallel-runway spacing is safe for a particular pair of aircraft. Current separation standards assume that spacings of greater than 2500 feet are safe for any pair of aircraft, e.g., a B-747-400 and a PA-28. Presumably, a smaller spacing would be safe for less disparate aircraft sizes, e.g., B-757 and B-737.

A first step[1] in such an analysis used GWVSS data to develop a model for vortex transport between parallel runways. The next step would be to extend the model to use MAVSS data, where vortex strength can be used explicitly to couple the model to a vortex encounter model.

Existing studies have not yet assessed the effect of wind sensor location on the correlation of wake vortex motion with the measured crosswind. The anemometer used to measure the crosswind in the O'Hare study was located quite far from the location of the vortex sensors. Using the GWVSS anemometers to measure the ambient crosswind may give better correlation with vortex motion and thereby provide some indication of how ambient wind sensor location affects the prediction of wake vortex motion. Since recovering the O'Hare GWVSS data to derive ambient crosswind information would require substantial effort, this analysis will likely use one of the newer GWVSS datasets, e.g., DFW.

47

This page intentionally blank

APPENDIX A - VORTEX SENSING SYSTEMS

A.1 MAVSS

A.1.1 Operating Principle

The acoustic system (MAVSS) consists of a linear array of acoustic antennae. A short acoustic pulse is transmitted vertically upwards in a narrow beam, the signal is scattered by temperature fluctuations in the atmosphere, and the return signal is analyzed for doppler shifts. Each pulse provides a vertical profile of the vertical wind component. Since the ambient wind has little vertical component near the ground, the sensor is particularly sensitive to wake vortices that have substantial vertical wind components. The maximum height sensed was set at 200 feet for landing and 300 feet for takeoff. Since the MAVSS antenna does not scan, a vortex must move through the fixed vertical beam in order to be measured. Thus, the MAVSS is well suited for the present study of vortex transport from one runway to another, but not so well suited for an analysis of stalled vortices.

A.1.2 Data Recording

The MAVSS data were recorded on 14-channel audio recorders using one-inch recording tape. Ten channels were used for the MAVSS acoustic signals and the others were used for timing, time code, aircraft type, and other logistical parameters.

A.1.3 Data Reduction

The spectral processing of the MAVSS data could take twice real time if more than six antennas had significant signals. The playback system consisted of three Ubiquitous® spectrum analyzers that can process two MAVSS channels (of different frequencies) each. The spectrum analyzers were interfaced to a minicomputer that generated run files of mean frequency and standard deviation for each range gate. Each run file was terminated when the next run starts. The run files were processed to detect vortices using a correlation method and a hard copy of the results was generated. The data for each detection was recorded in 80-character punched-card format. The consistency of the vortex detections was checked by eye and edited when needed to eliminate false detections.

A.2 GWVSS

A.2.1 Operating Principle

The ground-wind system (GWVSS) consists of lines of single-axis anemometers, installed perpendicular to the flight path. Each anemometer is mounted on a pole 10 feet above the ground. The anemometers are pointed perpendicular to the flight path so that the signal is proportional to the crosswind. The crosswind component produced by the two counter-rotating wake vortices increases or decreases the ambient crosswind level. When the vortices are near the ground, their locations can be identified by the anemometers having the highest and lowest signals.

The GWVSS is capable of identifying stalled vortices and was therefore invaluable in providing data for the single runway problem, i.e., where vortices (generated by an aircraft landing or taking off) may have stalled on the runway centerline and thus represent a potential hazard to the next aircraft that uses the runway. However, for the parallel runway problem addressed in this study, the GWVSS has

several disadvantages. Under conditions of high crosswind (e.g., above 10 knots) or gusty winds, there is too much noise on the anemometer signal to give reliable vortex locations. Also, if the vortex is too high (e.g., more than 30 m above the ground), vortex detection becomes unreliable. Thus, the GWVSS signal from a wake vortex may be lost before the vortex decays because of a rise in vortex height or a change in the ambient crosswind. On the other hand, if the vortex is generated at a high enough height (e.g., on takeoff), it may never descend low enough to be detected by the GWVSS.

The O'Hare takeoff data collection effort deployed four lines of GWVSS anemometers; only Line 2 will be used in this study because it was adjacent to the MAVSS line and therefore enables direct comparisons between the two sensing systems. The actual distances of the sensors (GWVSS and MAVSS) from the runway centerline are listed in Table 2. The landing GWVSS installation was designed to study stalled wake vortices and was therefore too limited in extent to be used for lateral transport analysis.

A.2.2 Data Recording

The GWVSS anemometer data was digitized at 16 Hz in the field and transmitted to a data collection trailer, where it was recorded on digital magnetic tape at the full data rate by a minicomputer.

A.2.3 Data Reduction

A minicomputer was also used to process the data. The anemometer readings were processed in two-second blocks and plotted on a line-printer plot that showed the locations of the highest and lowest crosswind readings and the consistency of the highest and lowest locations. The plot lasted only until the arrival of the next aircraft at the GWVSS line(s). The line-printer plots were then analyzed visually to assess the vortex parameters, particularly the vortex death time and death position of each vortex.

APPENDIX B - O'HARE LANDING DATABASE

B.1 RUNLA

Table 27 lists the fields of RUNLA.

Table 27. Fields of RUNLA Table

Name	Type	Description	Case 1	Case 2
RECID	A17*	Date & Time	76-07-15:11:06:14	76-07-15:11:08:34
RUN	N*	GWVSS Run Number by tape	51	52
YEAR	A3	Year	76	76
GDAYNO	A3	Julian Day	198	198
GTIME	A8	GWVSS Arrival Time	11:06:14	11:08:34
MTIME	A8	MAVSS Arrival Time	11:06:14	11:08:34
MRUNNO	A3	MAVSS Run Number	51	52
RUNWAY	A6	Arrival Runway	32L1	32L1
FSTAT*	A5	Octal failure status word	0214	0214
WVSTAT*	A5	Octal W/V status word	0152	0152
RGYNO	N	Number of Red/Green/Yellow VAS status changes since start of last run (default=-1)	0	0
VASRGY	A2	VAS Light (Red, Yellow or Green)	R	R
DISPT	N	Displacement of Start of Run (seconds)	blank	blank
MDETNO	N	Number of MAVSS Vortex Detections (0 means MAVSS operational but no vortex detections)	2	2
NOP	N	Number of MAVSS Port Vortex Detections	1	2
NOS	N	Number of MAVSS Starboard Vortex Detections	1	0
ANOM	A2	Anomaly Flag (see below)	0	0
ACLETT	A1	Aircraft series letter (usually blank)	blank	blank
ACTYPE	A9	Aircraft Type	DC-8 H	727
ACNO	A2	Aircraft Code Number	12	2
AL	A4	Airline	DL	blank
AIRFL	A4	Flight Number	938	blank
ACWT	N	Aircraft Weight (klbs)	210	blank
Page2	A1	Used for database conversion	blank	blank
Page3	A1	Used for database conversion	blank	blank
Page4	A1	Used for database conversion	blank	blank

*FSTAT and WVSTAT refer to the status of the data collection system.

B.1.1 Vortex Advisory System (VAS)

The VAS[4] assessed wake vortex safety for landings based on the ambient wind. The VAS output consisted of three colors at the time of this analysis:

1. Green - wind strong enough that reduced separations are safe.

2. Red - wind too weak to permit reduced separations.

3. Yellow - warns that a change may be coming

B.1.2 Anomaly Flag

0. None

1. A vortex has crossed over the centerline (i.e., it has been detected on both sides of the centerline).

2. A vortex was moving *toward* the centerline (i.e., was backing up).

3. A vortex velocity of more than 10 m/s was recorded.

4. The port and starboard vortices from this aircraft have 'crossed over' (moving out to the starboard and port sides, respectively).

B.2 METLA

Table 28 lists the fields of METLA.

Table 28. Fields of METLA Table

Name	Type	Description	Case 1	Case 2
RECID	A17*	Date & Time	76-07-15:11:06:14	76-07-15:11:08:34
RUN	N*	GWVSS Run Number	51	52
TWR	A2	Wind Tower	1	1
WEATH	A4	Weather	C	C
PRESS	N	Barometric Pressure	1004.6	1004.7
TURB	N	Turbulence	0.7	0.7
TEMP	N	Temparature	19	19
U	N	Headwind (knots)	14.9	14.7
V	N	Crosswind (knots)	-1.3	-2.9

B.3 GWLA

Table 29 lists the fields of GWLA.

Table 29. Fields of GWLA Table

Name	Type	Description	Case 1	Case 2
RECID	A17*	Date & Time	76-07-15:11:06:14	76-07-15:11:08:34
RUN	N*	GWVSS Run Number	51	52
CASENO	N	Case Number	53	54
PRESDT	N	Port Vortex Residence Time (s)	20	18
PDEATH	A1	Port vportex Death Time (s)	blank	blank
SRESDT	N	Starboard Vortex Residence Time (s)	58	56
SDEATH	A1	Starboard Vortex Death Time (s)	*	*
K	A4		blank	blank
J	A4		J	blank

B.4 DETECTLA

Table 30 lists the fields of DETECTLA.

Table 30. Fields of DETECTLA Table

Name	Type	Description				
RECID	A17*	Date & Time	Case 1	Case 1	Case 2	Case 2
RUN	N*	GWVSS Run Number	51	51	52	52
VPORS	A1*	Starboard or Port Vortex	P	S	P	P
DTCTNO	A1*	Vortex Detection Number	1	1	1	2
SN	A2	Antenna Number	5	6	5	4
SD	N	Lateral Position (m)	-63	63	-63	-122
VN	A2	Vortex Number (1 or 2)	1	1	1	1
VT	N	Vortex Age (s)	20.8	38.8	14	37.2
VV	N	Vortex Transport Speed (m/s)	2	1.6	2.5	2.5
VH	N	Vortex Height (m)	22	24	32	17
RG	N	Range Gate	5	6	8	4
V05	N	5-m average Circulation (m^2/s)	-60	-72	-36	-20
V10	N	10-m average Circulation (m^2/s)	-72	-114	-76	-38
V20	N	20-m average Circulation (m^2/s)	0	0	-116	-56
V30	N	30-m average Circulation (m^2/s)	0	0	0	-70
C1	N	1st correlation (range band)	-94	-79	-55	-34
C2	N	2nd correlation (range gate)	125	121	84	43
VDC	N	Number detections for transport speed	2	1	2	2

This page intentionally blank

APPENDIX C - O'HARE TAKEOFF DATABASE

C.1 RUNTO

Table 31 lists the fields of RUNTO.

Table 31. Fields of RUNTO Table

Name	Type	Field Description	Case 1	Case 2
RECID	A17*	Date & Time	80-04-21:10:16:45	80-04-21:10:18:43
RUN	N*	GWVSS Run Number	71	72
GNAME	A10	GWVSS Tape Name	DAW043.GW	DAW043.GW
YEAR	A3	Year	80	80
GDAYNO	A3	Julian Day	112	112
GTIME	A8	GWVSS Takeoff Time	10:16:45	10:18:43
MTIME	A8	MAVSS Takeoff Time	10:16:50	10:18:43
MTAPE	A4	MAVSS Tape Number	7011	7011
DAWNO	A3	GWVSS Tape Number	43	43
MRUNNO	A3	MAVSS Run Number	71	72
MDAYNO	A3	MAVSS Julian Day	112	112
SEQNO	A3	Sequence Number	58	59
MDETNO	N	Number of MAVSS Vortex Detections	4	1
NOP	N	Number of MAVSS Port Vortex Detections	2	0
NOS	N	Number of MAVSS Starboard Vortex Detections	2	1
ANOM	A2	Anomaly Flag	0	0
ACTYPE	A9	Aircraft Type	DC-10	727
ACNO	A2	Aircraft Type Code	7	2
AL	A4	Airline	UA	UA
ATT	A3	Attitude at Line A	AB	OG
HL1	N	Height at Line 1 (ft)	125	50
HL2	N	Height at Line 2 (ft)	225	100
HL3	N	Height at Line 3 (ft)	350	200
PACTYPE	A8	Preceding Aircraft type	727	DC-10
PREVT	N	Time after preceding departure (s)	74	114
FACTYPE	A8	Following Aircraft Type	727	727
NEXTT	N	Time until following departure (s)	114	63
Page2	A1	Used for database conversion	blank	blank
Page3	A1	Used for database conversion	blank	blank
Page4	A1	Used for database conversion	blank	blank

C.2 METTO

Table 32 lists the fields of METTO.

Table 32. Fields of METTO Table

Name	Type	Field Description	Case 1	Case 2
RECID	A17*	Date & Time	80-04-21:10:16:45	80-04-21:10:18:43
RUN	N*	GWVSS Run number	71	72
TWR	A2	Tower for Wind Measurement	1	1
METTIME	N	Meteorological time	63.4	56
WEATH	A5	Sky conditions	S/20	S/20
PYR	N	Pyranometer reading	810	794
TEMP	N	Temperture	-25	-25
U	N	Headwind (knots)	8.6	6.7
V	N	Crosswind (knots)	6	6
VASM30	A1	VAS Light (Red or Green) 30-s before SOR	R	R
UM30	N	Headwind (knots) 30 s before SOR	11	8
VM30	N	Crosswind (knots) 30 s before SOR	5	5
GUSTM30	N	Wind Gust (knots) 30 s before SOR	0	0
VASSOR	A1	VAS Light at start of run (SOR)	R	R
USOR	N	Headwind (knots) at SOR	10	7
VSOR	N	Crosswind (knots) at SOR	6	6
GUSTSOR	N	Wind Gust (knots) at SOR	0	0
VAS30	A1	VAS Light 30 s after SOR	R	R
U30	N	Headwind (knots) 30 s after SOR	9	7
V30	N	Crosswind (knots) 30 s after SOR	6	7
GUST30	N	Wind Gust (knots) 30 s after SOR	0	0
VAS60	A1	VAS Light 60 s after SOR	R	R
U60	N	Headwind (knots) 60 s after SOR	9	6
V60	N	Crosswind (knots) 60 s after SOR	6	6
GUST60	N	Wind Gust (knots) 60 s after SOR	0	0
Wmag	N	Wind Magnitude (knots)	10.5	9

C.3 GWTO

Table 33 lists the fields of GWTO.

Table 33. Fields of GWTO Table

Name	Type	Description	Case 1	Case 2
RECID	A17*	Date & Time	80-04-21:10:16:45	80-04-21:10:18:43
RUN	N*	GWVSS Run Number	71	72
RUNREC	N	Run Record Number	3925	3978
CASENO	A2	Case Number	70	71
RESS1	N	Line 1 Starboard Vortex Residence Time (s)	18	14
RESS2	N	Line 2 Starboard Vortex Residence Time (s)	14	18
RESS3	N	Line 3 Starboard Vortex Residence Time (s)	0	0
RESP1	N	Line 1 Port Vortex Residence Time (s)	64	0
RESP2	N	Line 2 Port Vortex Residence Time (s)	44	-1
RESP3	N	Line 3 Port Vortex Residence Time (s)	0	0
DPS1	N	Line 1 Starboard Vortex Death Position (ft)	500	250
DPS2	N	Line 2 Starboard Vortex Death Position (ft)	300	300
DPS3	N	Line 3 Starboard Vortex Death Position (ft)	-1	-1
DPP1	N	Line 1 Port Vortex Death Position (ft)	150	-1
DPP2	N	Line 2 Port Vortex Death Position (ft)	350	200
DPP3	N	Line 3 Port Vortex Death Position (ft)	-1	-1
DTS1	N	Line 1 Starboard Vortex Death Time (s)	48	20
DTS2	N	Line 2 Starboard Vortex Death Time (s)	34	28
DTS3	N	Line 3 Starboard Vortex Death Time (s)	0	0
DTP1	N	Line 1 Port Vortex Death Time (s)	64	0
DTP2	N	Line 2 Port Vortex Death Time (s)	64	48
DTP3	N	Line 3 Port Vortex Death Time (s)	0	0
SV1FT30	N	Line 1 Starboard Vortex Position (ft) at 30 s	350	1200
SV1FT60	N	Line 1 Starboard Vortex Position (ft) at 60 s	1500	250
SV1FT90	N	Line 1 Starboard Vortex Position (ft) at 90 s	1000	-1
SV1FT120	N	Line 1 Starboard Vortex Position (ft) at 120 s	-1	-1
SV2FT30	N	Line 2 Starboard Vortex Position (ft) at 30 s	300	1200
SV2FT60	N	Line 2 Starboard Vortex Position (ft) at 60 s	1100	-1
SV2FT90	N	Line 2 Starboard Vortex Position (ft) at 90 s	600	-1
SV2FT120	N	Line 2 Starboard Vortex Position (ft) at 120 s	-1	-1
SV3FT30	N	Line 3 Starboard Vortex Position (ft) at 30 s	600	50
SV3FT60	N	Line 3 Starboard Vortex Position (ft) at 60 s	1200	-1
SV3FT90	N	Line 3 Starboard Vortex Position (ft) at 90 s	600	-1
SV3FT120	N	Line 3 Starboard Vortex Position (ft) at 120 s	-1	-1
PV1FT30	N	Line 1 Port Vortex Position (ft) at 30 s	50	-150
PV1FT60	N	Line 1 Port Vortex Position (ft) at 60 s	150	600
PV1FT90	N	Line 1 Port Vortex Position (ft) at 90 s	350	-1
PV1FT120	N	Line 1 Port Vortex Position (ft) at 120 s	-1	-1
PV2FT30	N	Line 2 Port Vortex Position (ft) at 30 s	100	100
PV2FT60	N	Line 2 Port Vortex Position (ft) at 60 s	350	-1
PV2FT90	N	Line 2 Port Vortex Position (ft) at 90 s	350	-1
PV2FT120	N	Line 2 Port Vortex Position (ft) at 120 s	-1	-1
PV3FT30	N	Line 3 Port Vortex Position (ft) at 30 s	-350	-400
PV3FT60	N	Line 3 Port Vortex Position (ft) at 60 s	-500	-1
PV3FT90	N	Line 3 Port Vortex Position (ft) at 90 s	1800	-1
PV3FT120	N	Line 3 Port Vortex Position (ft) at 120 s	-1	-1

C.4 DETECTTO

Table 34 lists the fields of DETECTTO.

Table 34. Fields of DETECTTO Table

Name	Type	Description					
RECID	A17*	Date & Time	Case 1	Case 1	Case 1	Case 1	Case 2
RUN	N*	GWVSS Run Number	71	71	71	71	72
VPORS	A1*	Vortex (Port or Starboard)	P	P	S	S	S
DTCTNO	A1*	Detection Number	1	2	1	2	1
SN	A2	Antenna Number	5	6	5	6	5
SD	N	Lateral Position (m)	61	91	61	91	61
VN	A2	Vortex Number (1 or 2)	2	2	1	1	1
VT	N	Vortex age (s)	36.6	44.4	21.6	30.6	17.4
VV	N	Vortex Transport Speed (m/s)	3.9	3.9	3.4	3.4	3.5
VH	N	Vortex Height (m)	37	29	43	41	14
RG	N	Range Gate	6	5	7	7	2
V05	N	5-m average circulation (m^2/s)	76	72	-53	-57	-37
V10	N	10-m average circulation (m^2/s)	160	146	-134	-120	-49
V20	N	20-m average circulation (m^2/s)	271	224	-224	-216	-81
V30	N	30-m average circulation (m^2/s)	339	273	-322	-286	-121
C1	N	1st correlation (band)	77	67	-66	-68	-24
C2	N	2nd correlation (range gate)	122	108	119	118	55
VDC	N	Number of detections for transport speed	2	2	2	2	1
Circ	N	Circulation (m^2/s)	382	302	-314	-312	-113
VVkts	N	Vortex Transport Speed (knots)	7.5	7.5	6.5	6.5	6.7

REFERENCES

[1] Yarmus, J.S., Burnham, D.C. and Hallock, J.N., "Motion of Aircraft Wake Vortices in Ground Effect," unpublished.

[2] Yarmus, J., Burnham, D., Wright, A. and Talbot, T., "Aircraft Wake Vortex Takeoff Tests at O'Hare International Airport," DOT/FAA/RD-94-25, August 1994, USDOT/Volpe National Transportation Systems Center, Cambridge, MA.

[3] Hallock, J.N., Winston, B.P., Burnham, D.C., Sullivan, T.E., McWilliams, I.G. and Wood, W.D., "Joint US/UK Vortex Tracking Program at Heathrow International Airport, Vol. II: Data Analysis," FAA-RD-76-58,II, September 1976, DOT/Transportation Systems Center, Cambridge, MA.

[4] Hallock, J.N. and Eberle, W.R. (editors), "Aircraft Wake Vortices: A State-of-the-Art Review of the United States R&D Program," FAA-RD-77-23, February 1977, DOT/Transportation Systems Center, Cambridge, MA.

[5] Sullivan, T.E., Hallock, J.N. and Winston, B.P., "Analysis of Ground-Wind Vortex Sensing System Data from O'Hare International Airport," FAA-RD-80-133, September 1980, DOT/Transportation Systems Center, Cambridge, MA.

[6] Winter, H. "Research and Development for a Wake Vortex Warning System in Germany," Report No. DOT/FAA/SD-92/1.1, Proceedings of the Aircraft Wake Vortices Conference, Washington, DC, October 29-31, 1991, pp. 3-(1-7).

[7] Burnham, D.C., "Chicago Monostatic Acoustic Vortex Sensing System, Volume I: Data Collection and Reduction," FAA-RD-79-103,I, October 1979, DOT/Transportation Systems Center, Cambridge, MA.

[8] Burnham, D.C. and Hallock, J.N., "Chicago Monostatic Acoustic Vortex Sensing System, Volume II: Decay of B-707 and DC-8 Vortices," FAA-RD-79-103,II, September 1981, DOT/Transportation Systems Center, Cambridge, MA.

[9] Sullivan, T., Hallock, J., Winston, B., McWilliams, I. and Burnham, D., "Aircraft Wake Vortex Takeoff Tests at Toronto International Airport," FAA-RD-78-143, February 1979, DOT/Transportation Systems Center, Cambridge, MA.

[10] Tetzlaf, G., Franke, J. and Schilling, V., "Wake Vortex Propagation in the Atmospheric boundary Layer," Report No. DOT/FAA/SD-92/1.2, Proceedings of the Aircraft Wake Vortices Conference, Washington, DC, October 29-31, 1991, pp. 47-(1-19).

[11] Burnham, D.C., and Hallock, J.N., "Chicago Monostatic Acoustic Vortex Sensing System, Volume IV: Wake Vortex Decay," FAA-RD-79-103,IV, July 1982, DOT/Transportation Systems Center, Cambridge, MA.